

Cutoff Effects of Wilson Fermions in the Absence of Spontaneous Chiral Symmetry Breaking

A Numerical Study in the Schwinger Model

DIPLOMARBEIT

zur Erlangung des akademischen Grades
Diplomphysikerin (Dipl.-Phys.)
im Fach Physik

eingereicht an der
Mathematisch-Naturwissenschaftlichen Fakultät I
Humboldt-Universität zu Berlin

von
Magdalena Luz
geboren am 11.1.1977 in Göttingen

Präsident der Humboldt-Universität zu Berlin:

Prof. Dr. Hans Jürgen Prömel

Dekan der Mathematisch-Naturwissenschaftlichen Fakultät I:

Prof. Thomas Buckhout, PhD

Gutachter:

1. Prof. Dr. Michael Müller-Preussker
2. Prof. Dr. Ulrich Wolff

eingereicht am: 23. November 2005

Tag der mündlichen Prüfung: 15. Dezember 2005

Abstract

This work investigates the scaling of Wilson fermions in a set up without spontaneous chiral symmetry breaking (S χ SB).

Wilson fermions are a lattice regularization which is widely used in lattice simulations of Quantum Chromodynamics (QCD). In order to avoid the notorious fermion doubling problem, it contains a term which breaks chiral symmetry explicitly even in the massless limit. As a consequence, in simulations of QCD in large volume lattice artifacts which scale linear in the lattice spacing do appear. However, with the help of a spurionic lattice symmetry, it has been shown, that those effects are closely connected to the phenomenon of spontaneous chiral symmetry breaking. In the chiral limit of a theory where this phenomenon is absent, leading cutoff effects are of second order. At finite quark masses corrections of $O(am_q)$ do appear.

We confirmed this argument numerically by a scaling study in the two dimensional Schwinger model. We use two degenerate, dynamical Wilson fermions in our simulations, since this version of the model not only provides the flavor structure needed to define the spurionic symmetry but, more importantly, due to the Mermin-Wagner theorem, no S χ SB can occur.

Keywords:

Lattice field theory, Schwinger Model, Cutoff effects, Monte Carlo Simulation

Zusammenfassung

Die vorliegende Arbeit untersucht das Skalierungsverhalten von Wilsonfermionen in einem Modell ohne spontane Brechung der chiralen Symmetrie ($S\chi SB$).

Wilsonfermionen sind eine Regularisierung der fermionischen Wirkung, die in modernen Gittersimulationen der Quantenchromodynamik oft zur Anwendung kommt. Zur Umgehung der Fermionenverdopplung enthält sie einen Term, der selbst im masselosen Limes die chirale Symmetrie explizit bricht. Infolgedessen treten bei Simulationen der QCD in grossem Volumen Gitterartefakte auf, die linear mit dem Gitterabstand a skalieren.

Zur systematischen Beschreibung von Cutoffeffekten in der Feldtheorie auf dem Gitter führte Symanzik eine effektive Kontinuumstheorie ein [1]. Terme höherer Ordnung in a treten dort als zusätzliche Wechselwirkungsterme auf, die von Impulsen jenseits des Cutoff π/a erzeugt werden. Welche Terme erscheinen können, ist im Wesentlichen durch Symmetrieüberlegungen bestimmt: Die effektive Kontinuumstheorie muss invariant unter denselben Transformationen wie die Gittertheorie sein.

In Ref. [2] wurde eine so genannte “spurionischen” Symmetrie, die verschiedene (Wilson-) Regularisierungen miteinander verknüpft, in diese Betrachtung miteinbezogen. Es zeigt sich dann, dass im chiralen Limes einer Theorie ohne $S\chi SB$ die führenden Cutoffeffekte in der Wilsondiskretisierung zweiter Ordnung in a sind. Bei endlicher Quarkmasse kommen Effekte der Ordnung $O(am_q)$ dazu.

Diese Hypothese konnte hier erfolgreich numerisch getestet werden. Zur Überprüfung des Arguments wurde eine Skalierungsstudie in der zwei-dimensionalen Quantenelektrodynamik, dem sog. Schwinger Modell, mit zwei Massen entarteten Fermionen durchgeführt. Dieses Modell wurde als Testlaboratorium ausgewählt, da es sowohl über die nötige Flavor Struktur verfügt, als auch, infolge des Theorems vom Mermin und Wagner, keine spontane Brechung einer kontinuierlichen Symmetrie auftreten kann.

Vor diesem Hintergrund scheinen Skalierungsstudien im Schwinger Modell nur in sehr beschränktem Masse auf die QCD in grossem Volumen, wo die chirale Symmetrie spontan gebrochen ist, übertragbar zu sein.

Diese Arbeit ist folgendermassen aufgebaut: In den Kapiteln 2 und 3 wird zunächst eine kurze Einführung in die Physik des Schwinger Modells gegeben. Insbesondere wird im 3. Kapitel eine äquivalente bosonische Theorie vorgestellt, die Aufschluss über die Teilchen des Schwinger Modells geben kann.

Daraufhin wird das Modell auf dem Gitter formuliert und das oben angesprochene Argument veranschaulicht (4. Kapitel). In Kapitel 5 schliesslich werden die Details der Skalierungsstudie und die Ergebnisse der numerischen Simulation beschrieben.

Schlagwörter:

Gittereichtheorie, Schwinger Modell, Gitterartefakte, Monte Carlo simulation

Contents

| | | |
|----------|---|-----------|
| 1 | Introduction | 1 |
| 2 | The Schwinger Model | 3 |
| 2.1 | Euclidean Field Theory | 4 |
| 2.1.1 | Euclidean Correlation Functions | 5 |
| 2.2 | Dimensional Analysis and Renormalization Properties | 6 |
| 2.3 | Internal Symmetries of the Action | 9 |
| 2.3.1 | Gauge Symmetry | 9 |
| 2.3.2 | Chiral Symmetry | 10 |
| 2.3.3 | The Axial Anomaly | 12 |
| 2.3.4 | The Two Flavor Model | 15 |
| 2.3.5 | PCAC Relation | 16 |
| 2.4 | Confinement | 17 |
| 2.5 | Topology | 17 |
| 3 | Bosonization | 20 |
| 3.1 | The Free Massless Fermion | 20 |
| 3.2 | The Free Massless Scalar Field | 22 |
| 3.3 | The Free Massive Fermion | 24 |
| 3.4 | Bosonizing the Schwinger Model | 25 |
| 4 | The Schwinger Model on the Lattice | 30 |
| 4.1 | Formulation of the Lattice Theory | 30 |
| 4.1.1 | Fields on the Lattice | 30 |
| 4.1.2 | Wilson Gauge Action | 31 |
| 4.1.3 | Confinement | 32 |
| 4.1.4 | Fermions on the Lattice | 34 |
| 4.2 | Cutoff Effects | 36 |
| 4.2.1 | Cutoff Effects and Spontaneous Chiral Symmetry Breaking | 38 |

| | | |
|----------|---|-----------|
| 5 | Numerical Study | 44 |
| 5.1 | Simulations | 44 |
| 5.1.1 | Fermion Matrix | 44 |
| 5.1.2 | Hybrid Monte Carlo | 45 |
| 5.1.3 | Performance of the Algorithm | 47 |
| 5.2 | Scaling Test | 49 |
| 5.2.1 | Continuum Limit | 51 |
| 5.2.2 | Observables | 53 |
| 5.2.3 | Results of the Scaling Test | 56 |
| 6 | Conclusions | 60 |
| A | Conventions | 65 |
| A.1 | Indices | 65 |
| A.2 | γ Matrices | 65 |
| A.2.1 | Euclidean γ Matrices | 66 |
| B | Calculation of the Forces | 67 |
| C | Correlation Functions and Topological Charge | 69 |
| C.1 | Correlation Functions | 69 |
| C.1.1 | Flavor Triplet | 70 |
| C.1.2 | Flavor Singlet | 72 |
| C.2 | Topological Charge | 73 |

List of Figures

| | | |
|-----|--|----|
| 5.1 | Performance of the algorithm: Upper plot: Number of steps necessary in a trajectory of length 1 to reach an acceptance of 90%, and the number of CG iterations as a function of L/a . Below: Measure ν for the number of inversions of the fermion matrix Q needed to calculate an independent gauge configuration. | 48 |
| 5.2 | The maximal forces and their norm averaged over the volume as a function of L/a . The first plot shows the gauge and fermion forces as defined in appendix B. In the second, the gauge force is scaled by a factor of $\beta \propto (L/a)^2$ and in the third we give the fermion force normalized to its value at the coarsest lattice with $L/a = 16$ | 50 |
| 5.3 | Values of $m \cdot L$ for our lattices at the hopping parameters given in table 5.2 as a function of a/L . The circle corresponds to the simulation at $\kappa = 0.2529$ and $L/a = 32$ | 52 |
| 5.4 | Axial current correlator at $\beta = 8$, $\kappa = 0.2530$ and $L/a = 32$ | 54 |
| 5.5 | Effective π masses from the pseudo scalar density (dots) and the axial current (stars) correlators at $\beta = 8$, $L/a = 32$, $\kappa = 0.2530$ | 54 |
| 5.6 | Squared matrix elements at $\beta = 8$, $\kappa = 0.2530$ for the pseudo scalar (below) and the axial current (above) two point function. | 56 |
| 5.7 | Pion mass as a function of a/L . The symbols at $a/L = 0$ are the three values for the approximate continuum solutions given in eq. (3.31), evaluated at our value of the quark mass. The diamond at $L/a = 32$ is an interpolated value from the two runs at $\kappa = 0.2530$ and $\kappa = 0.2529$ | 57 |

| | | |
|-----|--|----|
| 5.8 | Scaling of $\Phi_\pi \cdot L$ as a function of $(a/L)^2$. The square is our continuum limit. The diamond slightly displaced from $L/a = 32$ is an interpolated value from the two runs at $\kappa = 0.2530$ and $\kappa = 0.2529$ respectively. The circle at $L/a = 32$ is from the run with $\kappa = 0.2530$. The interpolated value nearly matches the one from the run at $\kappa = 0.2530$, it does therefore not change our conclusions. The fit parameters given below are calculated with the value at $\kappa = 0.2530$ | 58 |
| 5.9 | The scaling of Φ_π plotted against a/L . The dashed line is a fit to a polynomial with a linear and a quadratic term. At $a/L = 0$ we give the continuum value of this fit (triangle) together with the one obtained from the fit with a term quadratic in a/L only (square). | 59 |

List of Tables

| | | |
|-----|--|----|
| 2.1 | Isospin quantum numbers | 15 |
| 2.2 | Meson operators. | 16 |
| 5.1 | Number of steps per trajectory and autocorrelation time of the plaquette needed to determine ν for the different lattices. The acceptance probability is also given. | 49 |
| 5.2 | Lattice parameters used in the simulations. | 52 |
| 5.3 | Simulation results for our observables at five different lattice spacings. | 57 |
| 5.4 | Fit parameters. | 59 |
| C.1 | Elements of the Fermion propagator \bar{S} and corresponding el- ements of $\gamma_0\bar{S}$ and $\bar{S}\gamma_0$ respectively. | 72 |

Chapter 1

Introduction

The goal of this thesis is to investigate the scaling behavior of Wilson fermions in the absence of spontaneous breaking of chiral symmetry ($S\chi SB$).

Wilson fermions are widely used in nowadays simulations of lattice QCD. This regularization solves the notorious fermion doubling problem by the introduction of a dimension 5 operator which becomes irrelevant in the continuum limit, but makes the doublers infinitely heavy at the same time. Its main drawback is however that the additional term explicitly breaks chiral symmetry. Thus, the symmetry is not realized at finite lattice spacing even in the limit of vanishing quark masses. In QCD, this is well known to introduce large cutoff effects which scale linear in the lattice spacing a [3] and can only be removed by including $O(a)$ counterterms.

Cutoff effects can be described in a systematic way by an effective continuum theory as proposed by Symanzik [1]. In this approach, the higher order terms in a appearing in the lattice action are interpreted as effective interactions generated by momenta above the cutoff. The lattice spacing a acts thereby as an effective coupling constant. Clearly, the terms appearing in such an expansion must respect the same symmetries as the original lattice theory.

Recently, an analysis of the Wilson action in terms of a so called “spurious” lattice symmetry, R_{sp}^5 , was proposed [2]. Apart from a chiral transformation of the fields, this symmetry also changes the sign of the Wilson and the mass term, connecting in this way different regularizations. Multiplicatively renormalizable operators can be classified into even or odd under R_{sp}^5 . By exploiting this fact, it becomes clear from the Symanzik expansion of such operators that in the chiral limit lattice artifacts of order a are tied to the spontaneous breakdown of chiral symmetry. In other words, if chiral symmetry is realized à la Wigner, chirally invariant operators are expected to approach their continuum limit at a rate proportional to a^2 .

We investigate this hypothesis by a numerical simulation of the Schwinger model. The system is implemented with two mass degenerate dynamical quark flavors. This provides the necessary flavor symmetries, such that the spurionic symmetry is well defined. More importantly, as a consequence of the Mermin Wagner theorem, no spontaneous breakdown of a continuous symmetry can occur in two dimensions.

Indeed, in agreement with our expectations, we find cutoff effects consistent with $O(a^2)$ only. In view of this result, scaling studies in the Schwinger model cannot simply be generalized to the phenomenologically very different case of QCD in large volume. For QCD in small volume however, a very similar pattern as the one observed here, might arise. This is currently under study in the Schrödinger functional [4, 5].

This work is organized as follows: we postpone the further discussion of the considerations sketched above to chapter 4. In the meantime, we have a closer look on our testing field, the Schwinger model. In chapter 2, we review some of its general properties. Chapter 3 introduces a method called bosonization, which is particular to two dimensions: at the level of correlations functions, fermionic theories are equivalent to bosonic ones. We motivate the method and introduce the bosonic theory, which corresponds to the Schwinger model in this sense. Although we do not make use of it in the numerical study, the equivalence is helpful to better understand the physics of the model.

In chapter 4 we return to our main issue. The Schwinger model is formulated on the lattice and the argument mentioned above presented in more detail. Chapter 5 finally focuses on the numerical study. In a first part we discuss the simulation algorithm and proceed then to explain the setup and the results of our scaling test.

Chapter 2

The Schwinger Model

For this study, we simulate the Schwinger model on the lattice. But before we turn to the numerical implementation we want to introduce the model in the continuum and discuss some of its most important properties.

The model describes a field theory in $1 + 1$ dimensions with an Abelian $U(1)$ gauge symmetry. It thus corresponds to QED in two space time dimensions. It was first introduced in 1962 by Schwinger in [6], where an analytic solution for the massless case was given. For the massive theory, however, no exact solution is known. In Minkowski space, the Lagrangian of the model is given by

$$\begin{aligned} \mathcal{L}[\bar{\psi}^a, \psi^a, A_\mu] &= \sum_{a=1}^{N_f} \bar{\psi}^a(x) [i\gamma^\mu \partial_\mu - g_0 \gamma^\mu A_\mu(x) - m_0] \psi^a(x) \\ &\quad - \frac{1}{4} F^{\mu\nu}(x) F_{\mu\nu}(x) = \\ &= \sum_{a=1}^{N_f} \bar{\psi}^a(x) [i\not{D} - m_0] \psi^a(x) - \frac{1}{4} F^{\mu\nu}(x) F_{\mu\nu}(x), \end{aligned} \tag{2.1}$$

where D_μ is the covariant derivative $\partial_\mu + ig_0 A_\mu$, ψ and $\bar{\psi} = \psi^\dagger \gamma_0$ are 2-spinors and $F_{\mu\nu}$ is the Abelian field strength tensor. The Lorentz indices μ and ν run over the values 0 and 1. In a two dimensional world, the field strength tensor is particularly simple. Since we have only one spatial direction, there is an electric field, but no orthogonal magnetic field can exist, so

$$F_{\mu\nu} = \partial_\mu A_\nu - \partial_\nu A_\mu = \begin{pmatrix} 0 & -E \\ E & 0 \end{pmatrix}.$$

In eq. (2.1), N_f labels the number of flavors. In principle, the model makes sense for any number of flavors, but we concentrate here on $N_f = 1$ and 2.

In the simulations, we used two mass degenerate flavors, partly for numerical reasons, but also because the argument we aim at checking numerically, depends on isospin symmetry. This explains our interest in the two flavor theory. However, for simplicity, we discuss those properties, which are common to both versions, in the one flavor model.

2.1 Euclidean Field Theory

The Lagrangian in eq. (2.1) defines the model in Minkowski space with the metric

$$g = \begin{pmatrix} 1 & 0 \\ 0 & -1 \end{pmatrix}.$$

Lattice simulations are done in the Euclidean path integral formulation of quantum field theories. So as a first step, we want to introduce that version of the model.

An introduction of the path integral can be found in many textbooks, as for instance refs. [7, 8]. In Minkowski space, it is defined by the

$$\mathcal{Z} = \int D\psi D\bar{\psi} DA_\mu e^{\frac{i}{\hbar} \int d^d x \mathcal{L}[\bar{\psi}, \psi, A_\mu]}. \quad (2.2)$$

We set $\hbar = 1$. The field variables are no longer operators, but classical fields which have to be anticommuting in the case of fermions. The quantum nature of the theory is accounted for by the summation over all possible field configurations with weight e^{iS} .

The integration measure in eqs. (2.2) needs a particularly careful definition. Since the fields are defined at every space time point and we integrate over all possible field configurations, there are infinitely many integration variables. Usually, the path integral is defined as the continuum limit of suitably defined lattice fields. To this end, we discretize a finite space time region through a lattice with lattice spacing a and points $x = (na)$, where n are sets of d integers ranging from $1, \dots, N_d$ each. $D\phi$ is then defined as

$$D\phi = \lim_{\substack{a \rightarrow 0 \\ L \rightarrow \infty}} \prod_n D\phi(na). \quad (2.3)$$

The weighting factor in eq. (2.2) is an oscillating function. This makes it unsuitable for numerical investigations. However, it is possible to bypass this problem by rotating the time axis by an angle of $\pi/2$. That is, we switch from t to the imaginary time it . Mathematically, this is equivalent to an analytical continuation of the theory in the complex plane. Under this so

called Wick rotation, $x_\mu x^\mu = t^2 - \mathbf{x}^2$ changes to $-t^2 - \mathbf{x}^2 = -x_E^2$ and the metric becomes Euclidean. In practice, we make the following substitutions:

$$t \rightarrow it \quad \partial_0 \rightarrow -i\partial_0 \quad A_0 \rightarrow -iA_0, \quad (2.4)$$

the last two corresponding to $D_0 \rightarrow -iD_0$, and we choose Euclidean γ matrices according to

$$\gamma_0^E = \gamma_0 \quad \text{and} \quad \gamma^E = -i\gamma. \quad (2.5)$$

The Euclidean matrices are hermitian and obey the relation

$$\{\gamma_\mu^E, \gamma_\nu^E\} = 2\delta_{\mu\nu}. \quad (2.6)$$

The exact two dimensional representation of the γ matrices, which we use in our simulation, can be found in appendix A.

With these replacements we obtain the *Euclidean action* S_E of the Schwinger model

$$\begin{aligned} iS_E &= i \int d^2 x_E \mathcal{L}_E \\ &= i \int d^2 x_E \bar{\psi} [\gamma_0^E \partial_0 + \gamma_1^E \partial_1 + ig_0(\gamma_0^E A_0 + \gamma_1^E A_1) + m_0] \psi + \frac{1}{4} F_{\mu\nu} F_{\mu\nu}, \end{aligned} \quad (2.7)$$

where the sum over flavor has been omitted. Substituting S by iS_E in the path integral in eq. (2.2) leads to a real weight factor, which exponentially damps configurations with large action

$$\mathcal{Z}_E = \int D\psi D\bar{\psi} DA_\mu e^{-S_E}. \quad (2.8)$$

Technically, \mathcal{Z}_E is the field theoretic analogue to the partition function of statistical mechanics. From now on, if not stated otherwise, we will assume to be working in Euclidean space. We therefore omit the index E .

2.1.1 Euclidean Correlation Functions

Consider the vacuum expectation value of an operator \mathcal{O}

$$C(t - t_0) = \langle 0 | \mathcal{O}(t) \mathcal{O}(t_0) | 0 \rangle = \langle 0 | e^{Ht} \mathcal{O}(0) e^{-Ht} \mathcal{O}(0) | 0 \rangle, \quad (2.9)$$

where we used the Euclidean time evolution of \mathcal{O} in the second step and set $t_0 = 0$ for convenience. If we insert a complete set of energy eigenstates, eq. (2.9) becomes

$$C(t) = \sum_n |\langle 0 | \mathcal{O} | n \rangle|^2 e^{(E_0 - E_n)t} \xrightarrow{t \rightarrow \infty} |\langle 0 | \mathcal{O} | 1 \rangle|^2 e^{-(E_1 - E_0)t}. \quad (2.10)$$

The states $|n\rangle$ depend on the quantum numbers of \mathcal{O} and n is meant to run over all excited states in the channel of \mathcal{O} . As we take the infinite time limit, the higher contributions are suppressed and the decay of $C(t)$ becomes dominated by the mass gap of the theory, $m = E_1 - E_0$, where E_0 is the vacuum energy. Note that eq. (2.9) is the expectation value of a two point function. In statistical mechanics its decay is governed by the correlation length ξ of the system. So by analogy, we see from eq. (2.10) that the mass gap m is related to ξ as $m = \xi^{-1}$. Finally, if we impose periodic boundary conditions in time on a system with total time extent T , the correlator must be symmetric in $t \rightarrow T - t$. Therefore, we can write $C(t) = \frac{1}{2}(\langle 0|\mathcal{O}(t)\mathcal{O}(0)|0\rangle + \langle 0|\mathcal{O}(T-t)\mathcal{O}(0)|0\rangle)$, which can be evaluated along the same lines to

$$\begin{aligned} C(t) &= \sum_n |\langle 0|\mathcal{O}|n\rangle|^2 \frac{1}{2}(e^{-(E_0-E_n)t} + e^{-(E_0-E_n)(T-t)}) = \\ &= \sum_n |\langle 0|\mathcal{O}|n\rangle|^2 \frac{e^{-(E_0-E_n)T/2}}{2} (e^{-(E_0-E_n)(t-T/2)} + e^{-(E_0-E_n)(T/2-t)}) \\ &\xrightarrow{t \rightarrow T/2} |\langle 0|\mathcal{O}|1\rangle|^2 e^{-mT/2} \cosh(m(T/2-t)), \end{aligned} \tag{2.11}$$

where obviously the total extent T has to be chosen large enough.

2.2 Dimensional Analysis and Renormalization Properties

The Schwinger model is super-renormalizable by power counting. This means that in a perturbative expansion there exist only a finite number of divergent diagrams. Consequently, all divergences can be removed in order to obtain a physically meaningful, finite theory. We want to derive this result here. To this end, we will have to make a short digression into perturbation theory. In d dimensional spacetime the argument goes as follows:

Let us denote by $[\mathcal{O}]$ the mass dimension of the operator \mathcal{O} . The action $S = \int d^d x \mathcal{L}$ is dimensionless. Since dx has mass dimension -1 (and accordingly the derivative operator has $[\frac{\partial}{\partial x}] = 1$), the mass dimension of the Lagrangian is d . Hence, it follows from eq. (2.1) that $[F_{\mu\nu}^2] = d$, from which we can infer the dimension of the gauge field

$$[A_\mu] = \frac{d}{2} - 1.$$

In the same way, from the kinetic term of the fermionic action $\bar{\psi}(x)\not{\partial}\psi(x)$ we derive that

$$[\psi] = \frac{d-1}{2}.$$

Finally, by inserting these findings into the interaction term, the dimension of the coupling constant can be evaluated to

$$\delta = [g_0] = d - \left(\frac{d}{2} - 1\right) - (d-1) = 2 - \frac{d}{2}.$$

Thus, in the case of two dimensional spacetime, g_0 has dimension 1. This is an important result, as we will see that the renormalization properties of a theory can be classified by the dimension of its coupling constants.

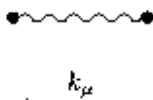
On the other hand, the superficial degree of divergence of a Feynman graph is given by the power of the momenta appearing in it. In order to determine this, we must have a look at the Feynman rules of QED. In Euclidean space they are as follows [9]:

- (i) Each internal fermion line carries a propagator



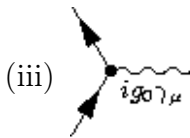
$$S_F(p) = -\frac{i}{\not{p} + m}$$

- (ii) To each internal photon line a photon propagator has to be attached



$$\Delta_{\mu\nu}(k) = \frac{1}{k^2}(\delta_{\mu\nu} + (\xi - 1)\frac{k_\mu k_\nu}{k^2}),$$

where the parameter ξ determines the chosen gauge.



To each vertex a factor of $i g_0 \gamma_\mu$ is associated and it carries a momentum conservation prescription $\delta(p_{\text{in}} - p_{\text{out}})$.

- (iv) Integrate over all loop momenta k_i not fixed by momentum conservation. Every integration contributes a factor $\int \frac{d^d k}{(2\pi)^d}$.
- (v) Multiply by a factor of -1 for each closed fermion loop.
- (vi) The diagram is multiplied by a symmetry factor which accounts for all topologically equivalent graphs.
- (vii) Attach the appropriate wave functions to external fermion and photon lines.

The last three rules have no influence on our argument and are merely given for completeness.

Let us now think of a diagram which has

- L : independent loops
- P_i / P_e : internal and external photon lines
- E_i / E_e : internal / external fermion lines
- V : vertices.

By rule (iv) we have an integration over $d^d k$ for each loop. This yields a momentum power of dL . From (i) and (ii) we see that every internal fermion line contributes a factor of p^{-1} and every internal photon line a power -2 . Therefore the superficial degree of divergence of the graph is

$$\omega = dL - 2P_i - E_i. \quad (2.12)$$

If $\omega \geq 0$, the diagram is said to be superficially divergent, because, it scales at least logarithmically, as we integrate over the momenta up to infinity.

We want to express eq. (2.12) in terms of the number of vertices V , the dimension of the coupling δ and the number of external lines. This makes it easier to classify the theory, since by rule (iii) V determines the power of the coupling g_0 and therewith the order of the graph in perturbation theory.

There are two fermion and one photon line attached to every vertex, so we have

$$2V = 2E_i + E_e \quad V = 2P_i + P_e. \quad (2.13)$$

A single loop on which lie n vertices contributes n internal lines. If we add a second loop with m new vertices without generating an additional vertex on the first one, we get $m - 1$ additional internal lines, since they share one. By continuing in this way, until we have constructed all L loops, we see that the total number of internal lines $E_i + P_i$ is given by

$$P_i + E_i = L + V - 1.$$

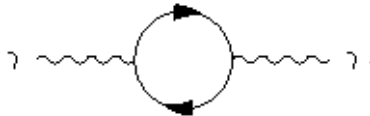
We use these three relations to eliminate P_i , E_i , L and d in eq. (2.12), which then reads

$$\omega = 4 - \delta(V + 2) - (1 - \delta)P_e - \left(\frac{3}{2} - \delta\right)E_e. \quad (2.14)$$

Now, if we think of a graph with a fixed number of external lines and increment its order in perturbation theory by adding more and more loops, we increase the number of vertices V . ω then depends crucially on the dimension of the coupling δ :

- If $\delta > 0$, ω decreases with increasing V for any given number of external lines. There exists only a finite number of divergent diagrams and the theory is super-renormalizable.
- For $\delta = 0$, ω does not depend on V ; the theory is renormalizable. This is true for the physically relevant quantum field theories in four dimensions, such as QCD, QED and the electroweak theory.
- Finally, for $\delta < 0$, ω increases with growing number of vertices. In a loop expansion, more and more divergent diagrams are generated; the theory is non-renormalizable.

Since the coupling of the Schwinger model has dimension 1, the theory belongs to the first group, as we have claimed at the beginning of this section. In fact, there is only one divergent diagram, which is the vacuum polarization graph [10]



2.3 Internal Symmetries of the Action

We proceed to discuss the internal symmetries of the action of the Schwinger model. By this we mean symmetries which do not imply a transformation of spacetime arguments. At first, we will restrict ourselves to the one flavor model. The features we introduce there, remain present anyway also in the case of two flavors. Then, in section 2.3.4 we extend the discussion to the additional properties resulting from a second flavor.

2.3.1 Gauge Symmetry

The theory is explicitly constructed with an invariance under a local phase shift

$$\psi(x) \rightarrow e^{i\alpha(x)}\psi(x) \quad \bar{\psi}(x) \rightarrow \bar{\psi}(x)e^{-i\alpha(x)}. \quad (2.15)$$

This makes the transition from the ordinary derivative ∂_μ to the covariant one D_μ in the Lagrangian mandatory. If we require $D_\mu\psi$ to transform in the same way as ψ itself, i.e.

$$D_\mu\psi' = e^{i\alpha(x)}D_\mu\psi,$$

we are forced to introduce a new physical degree of freedom, a real vector field A_μ , which in turn transforms like

$$A_\mu(x) \rightarrow A_\mu(x) - g_0^{-1} \partial_\mu \alpha(x). \quad (2.16)$$

The gauge field A_μ is massless, since a mass term would not be invariant under the above transformation. The field strength tensor $F_{\mu\nu}$ on the other hand, is gauge invariant due to the fact that $[\partial_\mu, \partial_\nu] = 0$. The gauge action $F_{\mu\nu} F^{\mu\nu}$ represents thus an invariant kinetic term for the gauge field. A_μ couples to the vector current $J_\mu(x) = \bar{\psi}(x) \gamma_\mu \psi(x)$, which is conserved by Noether's theorem

$$0 = \partial_\mu J^\mu = \partial_\mu (\bar{\psi} \gamma^\mu \psi). \quad (2.17)$$

2.3.2 Chiral Symmetry

In the chiral limit, i.e. at vanishing quark mass $m_0 = 0$, the Lagrangian acquires an additional symmetry. It becomes invariant under chiral rotations

$$\psi \rightarrow \exp(i\gamma_5 \alpha) \psi \quad \bar{\psi} \rightarrow \bar{\psi} \exp(i\gamma_5 \alpha), \quad (2.18)$$

such that the total symmetry group is $U(1)_A \times U(1)_V$. By Noether's theorem, chiral invariance is related to the conservation of the axial current

$$J_\mu^5(x) = \bar{\psi}(x) \gamma_\mu \gamma_5 \psi(x). \quad (2.19)$$

As an important side note we state at this point a very particular property of two dimensions: the vector- and the axial current are not independent, from the choice of the γ matrices (see appendix A) it follows that

$$i\gamma_5 \gamma_\mu = \epsilon_{\mu\nu} \gamma_\nu. \quad (2.20)$$

Here $\epsilon_{\mu\nu}$ is the total antisymmetric tensor in two dimensions and we set $\epsilon_{01} = 1$. In terms of the currents, this is equivalent to

$$J_\mu^5(x) = i\epsilon_{\mu\nu} J_\nu(x).$$

We will see that many properties of the Schwinger model depend on exactly this relation.

The two component spinor ψ can be expressed by γ_5 eigenstates

$$\psi = \begin{pmatrix} \psi_- \\ \psi_+ \end{pmatrix} \quad \text{with} \quad \gamma_5 \psi = \begin{pmatrix} -\psi_- \\ +\psi_+ \end{pmatrix}. \quad (2.21)$$

The operators

$$P_L = \frac{1}{2}(1 - \gamma_5) \quad \text{and} \quad P_R = \frac{1}{2}(1 + \gamma_5) \quad (2.22)$$

project to these states.

In the following, we want to introduce a notation for these chiral fields, which will prove useful in the next chapter, when we discuss the relation between bosons and fermions in two dimensions. To make the argument more transparent, we return to Minkowski space for a moment. Also we think of the fermions as operators such that we can make use of the notation $\bar{\psi} = \psi^\dagger \gamma_0$.

The massless Lagrangian in eq. (2.1) decouples into two independent parts for ψ_+ and ψ_-

$$\mathcal{L} = \psi_+^\dagger i(D_0 + D_1)\psi_+ + \psi_-^\dagger i(D_0 - D_1)\psi_-, \quad (2.23)$$

where we exploited the fact that $\gamma_0\gamma_1 = \gamma_5$. The Dirac structure disappeared completely from the Lagrangian. In the case of free fields, i.e. at $A_\mu = 0$, the equations of motion derived from eq. (2.23) are solved by the plain waves

$$\psi_+(x_+) = Ae^{i(p \cdot \mathbf{x} - \omega t)} = Ae^{ip_\mu x_+^\mu} \text{ and } \psi_-(x_-) = Ae^{i(p \cdot \mathbf{x} + \omega t)} = Ae^{ip_\mu x_-^\mu}, \quad (2.24)$$

with the space time arguments $x_\pm = (t, \pm \mathbf{x})$ and the momentum $p = (\omega, p)$. Thus, the field ψ_+ corresponds to a quark moving at speed of light to the right in spatial direction and ψ_- to a left-moving one. At this point we have to return to Euclidean space to pursue the argument. By doing the substitutions given in eq. (2.4), the fields ψ_- and ψ_+ can be expressed in terms of complex conjugate arguments i.e. $\psi_+(x) = \psi(x) = Ae^{ipx}$ and $\psi_-(x) = \psi(\bar{x}) = Ae^{ip\bar{x}}$ respectively, where $x = (it, \mathbf{x})$ and \bar{x} is its complex conjugate. They become analytic and anti-analytic functions of $x \in \mathbb{C}$ and the free Lagrangian equivalent to eq. (2.23) is

$$\mathcal{L} = \psi^\dagger(x) \frac{\partial}{\partial x} \psi(x) + \psi^\dagger(\bar{x}) \frac{\partial}{\partial \bar{x}} \psi(\bar{x}). \quad (2.25)$$

Since the left- and right-moving fermions do not mix, the two conserved currents (2.17) and (2.19) can be traded by a separate conservation law for each of them:

$$\partial_\mu (\bar{\psi} P_L \gamma^\mu \psi) = 0 \text{ and } \partial_\mu (\bar{\psi} P_R \gamma^\mu \psi) = 0. \quad (2.26)$$

Instead of the $U(1)_V \times U(1)_A$ symmetry group, we have $U(1)_R \times U(1)_L$. So the numbers of left- and right moving fermions seem to be conserved separately. But we will see in the next section that even though the massless action is invariant under chiral rotations, chiral symmetry is violated at the quantum level by an anomaly and the axial current in fact is not conserved.

2.3.3 The Axial Anomaly

The anomaly can be derived in various ways, including explicit calculation of loop integrals and current operator equations [11]. In the path integral formalism however it appears as a non-trivial Jacobian of the fermion integration measure [12, 11]. We will derive its exact form for the Schwinger model by shortly sketching this argument.

Suppose we shift the quark fields by an infinitesimal, local chiral transformation to

$$\psi' = (1 + i\alpha(x)\gamma_5) \psi \quad \text{and} \quad \bar{\psi}' = \bar{\psi} (1 + i\alpha(x)\gamma_5). \quad (2.27)$$

Here, $\alpha(x)$ is chosen such that it vanishes smoothly outside a finite spacetime region R . Since ∂_μ acts on α as well, eq. (2.27) leads to an additional term δS in the action, which after a partial integration can be written as the divergence of the axial current J_μ^5 ,

$$\int d^2x \bar{\psi}' \not{D} \psi' = \int d^2x [\bar{\psi} \not{D} \psi - i\alpha(x) \partial_\mu (\bar{\psi} \gamma_\mu \gamma_5 \psi)]. \quad (2.28)$$

Let \mathcal{O} be a product of local fields. The expectation value of \mathcal{O}

$$\langle \mathcal{O} \rangle = \frac{1}{\mathcal{Z}} \int D\bar{\psi} D\psi \mathcal{O} e^{-\int d^2x \bar{\psi} \not{D} \psi} \quad (2.29)$$

cannot be affected by a change of the integration variables as in eq. (2.27). Thus we must have

$$0 = \delta \langle \mathcal{O} \rangle = \langle \delta \mathcal{O} \rangle - \langle \mathcal{O} \delta S \rangle + \langle \mathcal{O} \delta \mathcal{J}^{-2} \rangle. \quad (2.30)$$

The last term arises if the integration measure does not transform in a trivial way, i.e. if the Jacobian \mathcal{J} in

$$D\psi' D\bar{\psi}' = \mathcal{J}^{-2} D\psi D\bar{\psi} \quad (2.31)$$

is different from $\mathbb{1}$.

If \mathcal{O} is localized outside the region R , then the shift in eq. (2.27) does not affect it and $\delta \mathcal{O}$ vanishes. Moreover, the product of fields in \mathcal{O} is arbitrary (as long as they are localized outside R), and thus we can conclude from eq. (2.30) that

$$\delta \mathcal{J}^{-2} - \delta S = 0. \quad (2.32)$$

Therefore in the present case, we get the classical conservation of the axial current, $\delta S = 0$, only if the Jacobian of the transformation in eq. (2.27) is

trivial. We will show in the following that in fact this is not what happens here.

Let φ_m be a complete set of eigenstates of the operator \mathcal{D} with eigenvalues λ_m . At vanishing A_μ the solutions of the problem $\mathcal{D}\mathcal{D}\varphi_m = \lambda_m^2\varphi_m$ are plain waves with definite momentum k_m and $\lambda_m^2 = -\omega_m^2 - k_m^2 < 0$. The k_m can become arbitrarily large, which makes it necessary to regularize the theory. To this end we introduce a hard momentum cutoff M , which we will take to infinity later on.

We write the fermion fields in the basis φ_m

$$\psi(x) = \sum_m c_m \varphi_m(x),$$

where the sum is truncated by the cutoff. The functional measure is given by $D\psi = \prod_m dc_m$. The transformed field ψ' becomes in this same basis

$$\psi' = \sum_m c'_m \varphi_m = \sum_{m,n} \langle \varphi_m | (1 + i\alpha\gamma_5) | \varphi_n \rangle c_n \varphi_m. \quad (2.33)$$

So by comparison, we get for the new coefficients c'_m

$$c'_m = \sum_n \langle \varphi_m | (1 + i\alpha\gamma_5) | \varphi_n \rangle c_n = \sum_n (\delta_{m,n} + i\alpha(x) T_{m,n}) c_n, \quad (2.34)$$

and the Jacobian \mathcal{J} of the transformation is given by

$$\det \mathcal{J} = \det (1 + i\alpha T) = e^{\text{tr} \log(1 + i\alpha T)}.$$

Since α is very small, we can expand the logarithm in the above expression, such that

$$\det \mathcal{J} = e^{i\alpha \text{tr} T + O(\alpha^2)} \quad \text{or} \quad \log \det \mathcal{J} = i\alpha \text{tr} T + O(\alpha^2), \quad (2.35)$$

with $\text{tr} T = \sum_n \langle \varphi_n | \gamma_5 | \varphi_n \rangle$. Remember that we still retain the momentum cutoff M . The regulator can be made explicit by writing $\text{tr} T$ as

$$\text{tr} T = \lim_{M^2 \rightarrow \infty} \sum_n \langle \varphi_n | \gamma_5 | \varphi_n \rangle e^{\lambda_n^2/M^2} = \lim_{M^2 \rightarrow \infty} \sum_n \langle \varphi_n | \gamma_5 e^{\mathcal{D}^2/M^2} | \varphi_n \rangle. \quad (2.36)$$

We remind that $\lambda_n^2 < 0$, so the theory really is properly regularized.

If we write the product $\gamma_\nu \gamma_\mu$ as

$$\gamma_\nu \gamma_\mu = \frac{1}{2} ([\gamma_\nu, \gamma_\mu] + \{\gamma_\nu, \gamma_\mu\}) = -i\sigma_{\nu\mu} + \delta_{\nu\mu},$$

the operator \mathbb{D}^2 in eq. (2.36) can be evaluated to $D^2 - i\sigma_{\mu\nu}D_\mu D_\nu$. The matrix $\sigma_{\mu\nu}$ introduced here is defined through the commutator of the γ matrices. In addition, in two dimensions it is proportional to γ_5 by the relation given in eq. (2.20):

$$\sigma_{\mu\nu} \equiv \frac{i}{2} [\gamma_\mu, \gamma_\nu] = \epsilon_{\mu\nu}\gamma_5. \quad (2.37)$$

In a next step, we write $D_\mu D_\nu$ explicitly as

$$D_\mu D_\nu = \partial_\mu \partial_\nu - g_0^2 A_\mu A_\nu + ig_0 \underbrace{(\partial_\mu A_\nu + A_\mu \partial_\nu)}_{(\partial_\mu A_\nu) + A_\nu \partial_\mu + A_\mu \partial_\nu}. \quad (2.38)$$

All terms except for $ig_0(\partial_\mu A_\nu)$ are symmetric in μ and ν and cancel upon multiplication with $\sigma_{\mu\nu}$; $ig_0(\partial_\mu A_\nu)$ on the other hand, can be replaced by the distinctly antisymmetric tensor $\frac{ig_0}{2}(\partial_\mu A_\nu - \partial_\nu A_\mu) = \frac{ig_0}{2}F_{\mu\nu}$. So finally, we can express the derivative operator in eq. (2.36) as

$$\mathbb{D}^2 = D^2 + \frac{g_0}{2}\sigma_{\mu\nu}F_{\mu\nu}.$$

Since D^2 acts only in position space and does not carry Dirac indices, eq. (2.36) can be written as the product of two traces, one in Dirac- and the other in position space

$$\lim_{M^2 \rightarrow \infty} \text{tr} \left[\gamma_5 \exp \left(\frac{g_0}{2M^2} \sigma^{\mu\nu} F_{\mu\nu} \right) \right] \int d^2x \langle [.2ex] | x e^{D^2/M^2} | [.2ex] \rangle x. \quad (2.39)$$

We proceed to evaluate the Dirac trace first. As we are only interested in the limit of large M^2 , the exponential can be expanded. The constant term vanishes because γ_5 is traceless and we get up to $O(1/M^4)$

$$\text{tr} \left[\gamma_5 \frac{g_0}{2M^2} \sigma_{\mu\nu} F_{\mu\nu} \right] = \frac{g_0}{M^2} \epsilon_{\mu\nu} F_{\mu\nu}. \quad (2.40)$$

Here, we used eq. (2.37) to substitute $\sigma_{\mu\nu}$ by γ_5 . The other trace in eq. (2.39) can best be evaluated in Fourier space. In the limit $M^2 \rightarrow \infty$, all but the largest k contributions are suppressed. We can therefore restrict ourselves to the terms proportional to k^2 , which means that we trade the covariant derivative D in eq. (2.39) for the ordinary one. The trace becomes then a Gaussian integral

$$\int d^2x \langle x | e^{\partial^2/M^2} | x \rangle = \int \frac{d^2k}{4\pi^2} e^{-k^2/M^2} = \frac{M^2}{4\pi}.$$

The transformation of the adjoint spinor $\bar{\psi}$ can be calculated in the very same way by defining left eigenvectors to \not{D} . It leads to another factor of $e^{i\alpha \text{ tr } T}$. So, eventually the Jacobian of the axial transformation (2.27) is

$$\det \mathcal{J}^2 = \exp \left(i \int d^2x \alpha \frac{g_0}{2\pi} \epsilon_{\mu\nu} F_{\mu\nu} \right). \quad (2.41)$$

Relating this to eq. (2.32), we see that, contrary to the expectations from the classical theory, the axial current conservation is spoiled by a term proportional to $F_{\mu\nu}$,

$$\partial_\mu J_\mu^5(x) = \frac{g_0}{2\pi} \epsilon_{\mu\nu} F_{\mu\nu}. \quad (2.42)$$

2.3.4 The Two Flavor Model

Up to now we have discussed the symmetries of the one flavor Schwinger model only. At this point, we want to enlarge our theory by adding a second quark flavor. The spinor ψ becomes a doublet, which we call (u, d) in analogy to QCD. We use the letters a, b, \dots to label flavor components. We confine ourselves to the case of degenerate masses, i.e. we set $m_u = m_d = m_0$. The flavors u and d form an isospin doublet with the quantum numbers given in table 2.1. The two flavor Lagrangian is invariant under transformations of the quark fields with a unitary matrix $U \in U(2)$. The symmetry group can

| flavor | I | I_3 |
|--------|---------------|----------------|
| u | $\frac{1}{2}$ | $\frac{1}{2}$ |
| d | $\frac{1}{2}$ | $-\frac{1}{2}$ |

Table 2.1: Isospin quantum numbers

be split to $U(2) = U(1) \times SU(2)$, where the $U(1)$ is gauged as in the one flavor case and the $SU(2)$ part is a global transformation which corresponds to a non-trivial rotation in flavor space

$$\psi \rightarrow e^{i\omega^a \frac{\tau^a}{2}} \psi \quad \bar{\psi} \rightarrow \bar{\psi} e^{-i\omega^a \frac{\tau^a}{2}}. \quad (2.43)$$

If we build quark bilinears $\frac{1}{2} \bar{\psi} \Gamma T \psi$ out of the doublet (u, d) , we get an isospin triplet with $I = 1$ and a singlet with $I = 0$. Here, Γ represents a product of γ matrices and T is a flavor matrix, either $\mathbb{1}$ for the singlet or one of the following for the triplet:

$$\tau^+ = \frac{1}{\sqrt{2}} (\sigma_1 + i\sigma_2), \quad \tau^- = \frac{1}{\sqrt{2}} (\sigma_1 - i\sigma_2), \quad \tau^0 = \sigma_3. \quad (2.44)$$

Compared to four dimensions, there exists only a limited number of independent meson operators due to the two dimensional relation in eq. (2.20). They are summarized in table 2.2.

| operator | flavor singlet | flavor triplet |
|-----------|---|--|
| S | $\frac{1}{2}\bar{\psi}\psi$ | $\bar{\psi}\frac{\tau^a}{2}\psi$ |
| P | $\frac{1}{2}\bar{\psi}\gamma_5\psi$ | $\bar{\psi}\gamma_5\frac{\tau^a}{2}\psi$ |
| J_μ^5 | $\frac{1}{2}\bar{\psi}\gamma_\mu\gamma_5\psi$ | $\bar{\psi}\gamma_\mu\gamma_5\frac{\tau^a}{2}\psi$ |

Table 2.2: Meson operators.

In the same way, the massless action becomes invariant under the non-trivial chiral flavor rotations

$$\psi \rightarrow \psi' = e^{i\omega^a \frac{\tau^a}{2} \gamma_5} \psi \quad \bar{\psi} \rightarrow \bar{\psi}' = \bar{\psi} e^{i\omega^a \frac{\tau^a}{2} \gamma_5} \quad (2.45)$$

in addition to the $U(1)_A$ symmetry of the one flavor model. By an argument completely analogous to the one given in section 2.3.2, the chiral- and the ordinary isospin transformations can be combined to transformations acting on the left- and the right moving particles, ψ_+ and ψ_- , separately. Therefore at $m_0 = 0$, the total symmetry group is $U(1)_V \times U(1)_A \times SU(2)_R \times SU(2)_L$, which breaks to $U(1)_V \times SU(2)_V$ if we add a mass term. Also, as in the one flavor theory, the axial $U(1)_A$ is always anomalous. Under the axial isovector transformation given in eq. (2.45), on the other hand, no anomaly appears. This can be seen from the following consideration: the analogue to eq. (2.33) under this transformation is

$$\psi' = \sum_{m,n} \langle \varphi_m | 1 + i\alpha \frac{\tau^a}{2} \gamma_5 | \varphi_n \rangle c_n \varphi_m. \quad (2.46)$$

While calculating the Jacobian, we have to take an additional trace in flavor space. But since only τ^a acts non-trivially on flavor, this amounts simply to a factor of $\text{tr } \tau^a = 0$ in eq. (2.39), and hence the Jacobian determinant is simply $\det \mathcal{J} = 1$.

2.3.5 PCAC Relation

We want to extend our discussion of chiral symmetry a bit and derive the so called PCAC (Partially Conserved Axial Current) relation. This relation provides us with a mean to determine the quark mass, that we will use in the analysis of the numerical data. We stay with the two flavor model. In

order to derive the relation, we again transform the fields by an infinitesimal local chiral rotation

$$\bar{\psi} \rightarrow \bar{\psi} (1 + i\alpha(x)\frac{\tau}{2}\gamma_5) \quad \psi \rightarrow (1 + i\alpha(x)\frac{\tau}{2}\gamma_5) \psi.$$

For simplicity, we use the non-anomalous isovector transformation, so that we need not care about any anomaly terms. At finite mass m_0 , chiral symmetry is explicitly broken by the mass term and the action of the chirally rotated fields picks up an additional term δS :

$$S[\bar{\psi}', \psi', A_\mu] = S[\bar{\psi}, \psi, A_\mu] + \delta S, \quad (2.47)$$

where δS is given by

$$\delta S = i \int d^2x \alpha(x) \left[-\partial_\mu \left(\bar{\psi}(x)\gamma_\mu\gamma_5\frac{\tau^a}{2}\psi(x) \right) + 2m_0\bar{\psi}(x)\gamma_5\frac{\tau^a}{2}\psi(x) \right]. \quad (2.48)$$

By the argument given in section 2.3.3, it follows that δS must vanish, and we conclude that

$$\partial_\mu J_\mu^{5a}(x) = 2m_0 P^a(x), \quad (2.49)$$

where $P^a(x)$ is the pseudo scalar density as given in table 2.2. By sandwiching the operator relation (2.49) between suitable states one can extract the quark mass

$$m_{PCAC} = \frac{1}{2} \frac{\langle 0 | \partial_\mu J_\mu^5 | \pi \rangle}{\langle 0 | P | \pi \rangle}. \quad (2.50)$$

2.4 Confinement

An Abelian gauge theory in two dimensions is confining. The argument can be made very nicely on the lattice, therefore we postpone it to section (4.1.3).

2.5 Topology

The topological structure can be investigated by seeking solutions of finite energy in the pure gauge theory. Thus, we are looking for gauge field configurations, where $F_{\mu\nu} \xrightarrow{|x| \rightarrow \infty} 0$. Clearly, this is the case for all configurations satisfying $A_\mu = 0$ at infinity. But since the field strength tensor is gauge invariant, any configuration which at infinity is a gauge transformation of $A_\mu = 0$ (a so called pure gauge), has the same property

$$A_\mu(x) = -g_0^{-1} \partial_\mu \phi(x) \quad \text{for } |x| \rightarrow \infty. \quad (2.51)$$

In two dimensions, $|x| \rightarrow \infty$ defines a circle S^1 with $r \rightarrow \infty$ and $\theta \in [0, 2\pi)$. Furthermore, from eq. (2.15), we see that the function $\phi(x)$ determines a mapping of spacetime elements x to elements of the gauge group $G = e^{i\phi(x)}$. Thus at infinity, all gauge transformations of the form eq. (2.51) map S^1 to $U(1)$

$$\begin{aligned} S^1 &\rightarrow U(1) \\ \phi : \theta &\mapsto G. \end{aligned} \quad (2.52)$$

Such mappings are characterized by the winding number ν , which groups them into different homotopy classes: every ϕ is homotopic to a mapping $\theta \mapsto e^{i(\nu\theta + \alpha)}$. Thus, ν is given by

$$\nu = \int_0^{2\pi} \frac{d\theta}{2\pi} \frac{-i}{G(\theta)} \frac{dG}{d\theta} \quad (2.53)$$

The transformation in eq. (2.51) can equally be written in terms of the group element G

$$A_\mu(x) = ig_0^{-1} G^{-1} \partial_\mu G \quad \text{for } |x| \rightarrow \infty. \quad (2.54)$$

In the following, we want to express eq. (2.53) through the gauge field A_μ in the whole volume. To this end, we define the current $I_\mu = \epsilon_{\mu\nu} A_\nu$. Whenever $A_\mu(x)$ is a pure gauge, the divergence of $I_\mu(x)$ vanishes. This defines a quantity, in our case the winding number or topological charge ν , which is conserved independent of the equations of motion, it is said to be topologically conserved.

Consider the integral

$$\int d^2x \partial_\mu I_\mu(x) = \int d^2x \partial_\mu \epsilon_{\mu\nu} A_\nu(x) = \int d^2x \epsilon_{\mu\nu} F_{\mu\nu}(x). \quad (2.55)$$

By Stokes' law eq. (2.55) can be turned into a surface integral at $|x| \rightarrow \infty$. We denote by V the whole spacetime volume, then

$$\int_{\partial V} I_\mu dx^\mu = \int_0^{2\pi} I_\theta d\theta, \quad (2.56)$$

since ∂V is a circle. By eq. (2.54), the θ component of I at $|x| \rightarrow \infty$ is equal to $ig_0^{-1} G^{-1} \partial_\theta G$ and we obtain

$$\int d^2x \partial_\mu I_\mu = -\frac{2\pi\nu}{g_0}. \quad (2.57)$$

From this we conclude that the winding number can be written as the volume integral over the field strength tensor

$$\nu = -\frac{g_0}{2\pi} \int d^2x \epsilon_{\mu\nu} F_{\mu\nu}. \quad (2.58)$$

If we compare this equation to the one we have derived for the axial anomaly in eq. (2.42), we see that, for the one flavor model, the integrated divergence of the axial current is equal to the negative topological charge

$$\nu = -\int d^2x \partial_\mu J_\mu^5(x) = -\frac{g_0}{2\pi} \int d^2x \epsilon_{\mu\nu} F_{\mu\nu}(x). \quad (2.59)$$

For gauge configurations of a given ν the Euclidean gauge action is bounded from below. In order to show this, we need the Schwartz inequality: Let $\psi_1(x)$ and $\psi_2(x)$ be two real integrable functions, then

$$\left[\int \psi_1(x) \psi_2(x) dx \right]^2 \leq \int [\psi_1(x)]^2 dx \int [\psi_2(x)]^2 dx. \quad (2.60)$$

We set $\psi_1(x) = -\frac{g_0}{2\pi} \epsilon_{\mu\nu} F_{\mu\nu}(x)$ and $\psi_2(x) = \mathbb{1}$ then

$$\nu^2 \leq \frac{g_0^2 V}{4\pi^2} \int d^2x [\epsilon_{\mu\nu} F_{\mu\nu}(x)]^2 = \frac{g_0^2 V}{4\pi^2} 8S_G, \quad (2.61)$$

where we used that $[\epsilon_{\mu\nu} F_{\mu\nu}]^2 = 2F_{\mu\nu} F_{\mu\nu}$. Thus, we get

$$S_G \geq \frac{\nu^2 \pi^2}{2g_0^2 V}. \quad (2.62)$$

The winding number can also be defined on the lattice. We give the definition in appendix C, for a discussion of the topology on the lattice we refer to [13].

Chapter 3

Bosonization

In two dimensions, there exists a fundamental connection between bosonic and fermionic theories in infinite volume. Expectation values of fermion theories can be reformulated in terms of averages over boson fields. This method is called bosonization [10]. Here, we will shortly introduce the technique and then apply it to the Schwinger model. Although we simulated the purely fermionic theory, as it was discussed in the last chapter, we think that this excursion is interesting in its own right, as it helps to understand better the physics of the model. In particular, from the bosonized version it is easy to see what particles the theory ought to contain.

We emphasize again that throughout this chapter we work in two dimensions and in Euclidean space. Also, we are a bit sketchy concerning renormalization where it does not affect the argument, for more details we refer to [10].

3.1 The Free Massless Fermion

First we consider the action of a free massless fermion

$$S^F[\bar{\psi}, \psi] = \int d^2x \bar{\psi}(x) \not{\partial} \psi(x). \quad (3.1)$$

The propagator is given by

$$\Delta^F(x-y) = \int \frac{d^2k}{(2\pi)^2} e^{ik(x-y)} \frac{\not{k}}{k^2} = -\not{\partial} \left(\frac{1}{4\pi} \log(y-x)^2 \right) = -\frac{1}{2\pi} \frac{1}{\gamma^\mu(x-y)_\mu}. \quad (3.2)$$

This expression is divergent for $(x-y) \rightarrow 0$, but for our argument we can think of keeping the distance finite. Moreover, it is possible to deal with these UV divergences; we refer to [10]. We write the fermion as γ_5 eigenstates $\psi_+(x)$

and $\psi_-(x)$. We need here the notation of the γ_5 eigenstates as analytic and anti-analytic functions of a complex spacetime argument $z^j = iz_0^j + z_1^j$, as it has been explained in section 2.3.2. Since the Lagrangian decouples the right- and left moving components (see eq. (2.23)), we can define a separate propagator Δ_+^F and Δ_-^F for each of them¹. For ψ_- for instance, it can be obtained from eq. (3.2) by replacing $\not{\partial} \rightarrow \frac{\partial}{\partial(z^i - z^j)}$

$$\Delta_-^F(z^i - z^j) = \langle \psi_-^\dagger(z^i) \psi_-(z^j) \rangle = \frac{-1}{2\pi(z^i - z^j)}. \quad (3.3)$$

The propagator for ψ_+ is just the same with the complex conjugate argument \bar{z}^j instead of z^j .

By the Wick theorem, a $2n$ - point correlation function of left moving quark fields becomes

$$\langle \prod_{j=1}^n \psi_-^\dagger(z^j) \psi_-(x^j) \rangle = \frac{1}{n!} \sum_{\substack{\text{permut.} \\ \text{of } j_k}} (-1)^p \prod_{k=1}^n \Delta_-^F(z^{j_k} - x^{j_k}). \quad (3.4)$$

Here, p is the parity of the permutation and keeps track of the anticommuting nature of the fermions. The right hand side of eq. (3.4) is the determinant of a complex $n \times n$ matrix M with components $M_{ij} = \Delta_-^F(x^i - z^j)$. Moreover, due to eq. (3.3), it has the structure of a Cauchy determinant which satisfies the identity

$$(-1)^{n+1} \det(z^i - x^i)^{-1} = \frac{\prod_{i < j} (x^i - x^j)(z^i - z^j)}{\prod_{ij} (z^i - x^j)}. \quad (3.5)$$

Let us construct the quark bilinears $\sigma_+ = \psi_-^\dagger \psi_+$ and $\sigma_- = \psi_+^\dagger \psi_-$. They correspond to the left (right) moving quark density. Furthermore, we point out for later usage that the scalar and the pseudo scalar density can be written as linear combinations of σ_+ and σ_- : $\bar{\psi}\psi = \sigma_+ + \sigma_-$ and $\bar{\psi}\gamma^5\psi = \sigma_+ - \sigma_-$. Because ψ_+ and ψ_- are decoupled, expectation values of products σ_+ and

¹We stick to the notation with the dagger as we used it in the operator formulation in the last chapter. Here, ψ^\dagger simply denotes Grassmann valued field which is independent of ψ .

σ_- factorize into

$$\begin{aligned} \langle \prod_{j=1}^n \sigma_+(z^j, \bar{z}^j) \sigma_-(x^j, \bar{x}^j) \rangle &= (-1)^n \langle \prod_{j=1}^n \psi_+^\dagger(\bar{z}^j) \psi_+(\bar{x}^j) \rangle \langle \prod_{j=1}^n \psi_-^\dagger(z^j) \psi_-(x^j) \rangle \\ &= - \left(\frac{1}{2\pi} \right)^{2n} \frac{\prod_{i<j} |z^i - z^j|^2 |x^i - x^j|^2}{\prod_{ij} |x^i - z^j|^2}, \end{aligned} \quad (3.6)$$

where we have used the equality (3.5) in the last step and the products $(x^i - x^j)(\bar{x}^i - \bar{x}^j)$ have been evaluated to give the norm squared. The factor $(-1)^n$ accounts for the permutations of ψ_+ or ψ_- .

3.2 The Free Massless Scalar Field

We leave the fermion for a moment and turn to a massless scalar field. We will derive an expression for correlation functions of exponentials of such a field which turns out to be equivalent to the correlation functions of the σ_\pm fields of the last section. More precisely, we want to investigate the expression

$$\langle \prod_{j=1}^n e^{i\kappa_j \phi(x_j)} \rangle_{S^S} = \int D\phi e^{-S^S[\phi] + i \sum_j \kappa_j \phi(x_j)} = \int D\phi e^{-\int d^2x [\mathcal{L}^S - J(x)\phi(x)]}, \quad (3.7)$$

where S^S is the action of a scalar

$$S^S[\phi] = \frac{1}{2} \int d^2x [(\partial_\mu \phi(x))^2 + m^2 \phi(x)^2] \quad (3.8)$$

at $m^2 = 0$. The reason for giving a mass term at all, is to avoid infrared divergences in the propagator. We will eventually take the limit $m \rightarrow 0$ with a suitable prescription. In eq. (3.7), we included the argument of the exponential on the lhs in the space time integral by writing it as a sum over point sources $J(x) = i \sum_j \kappa_j \delta(x - x_j)$.

Now, let ϕ_0 be the field

$$\phi_0(x) = \int \Delta^S(x - y) J(y) d^2y,$$

where Δ^S is the scalar field propagator. The configuration ϕ_0 is the solution to $(-\partial^2 + m^2)\phi_0(x) = J(x)$. By shifting $\phi \rightarrow \phi + \phi_0$ in eq. (3.7), we obtain a

Gaussian integral in ϕ which can be integrated out. So finally, we arrive at the expression

$$\left\langle \prod_{i=1}^n e^{\kappa_i \phi(x_i)} \right\rangle_{GS} = M e^{\int d^2x d^2y (J(x) \Delta^S(x-y) J(y))} = M e^{-\sum_{i,j} \kappa_i \kappa_j \Delta^S(x_i - x_j, m)} \quad (3.9)$$

with $M = (\det[-\partial^2 + m^2])^{-\frac{1}{2}}$. The spacetime integrations could be trivially evaluated because of the δ functions in the sources.

For small masses the scalar field propagator Δ^S is given by

$$\Delta^S(x_i - x_j, m) = \frac{1}{(2\pi)^2} \int d^2p \frac{e^{ip(x_i - x_j)}}{p^2 + m^2} = -\frac{1}{2\pi} \left(\log \frac{m(x_i - x_j)}{2} + \gamma \right) + O(m) \quad (3.10)$$

with the Euler constant γ [10]. Again, Δ^S is UV divergent as x_i approaches x_j . It can be regularized by introducing a momentum cutoff Λ [10] and the regularized propagator at 0 distance is

$$\Delta^S(0, m) = \frac{1}{4\pi} \log(\Lambda^2/m^2) + \text{const} + O(m). \quad (3.11)$$

We evaluate the argument of the exponential in eq. (3.9) by inserting the explicit expressions in eqs. (3.10) and (3.11). This yields up to $O(m)$

$$\begin{aligned} & -2\pi \sum_{i,j} \kappa_i \kappa_j \Delta(x_i - x_j, m) = \\ & = -2\pi \left[\sum_{i \neq j} \kappa_i \kappa_j \Delta(x_i - x_j, m) + \sum_i \kappa_i^2 \Delta(0, m) \right] = \\ & = \sum_{i \neq j} \kappa_i \kappa_j (\log |x_i - x_j| + \log m + c_1) + \sum_i \kappa_i^2 (\log m - \log \Lambda + c_2) = \\ & = \sum_{i \neq j} \kappa_i \kappa_j \log |x_i - x_j| - \sum_i \kappa_i^2 \log \Lambda + \left(\sum \kappa_i \right)^2 (\log m) + c_3. \end{aligned} \quad (3.12)$$

The c_j are just constants, irrelevant for the argument. The separation $(x_i - x_j)$ appears only in logarithms, thus upon exponentiating eq. (3.12), the expectation value in eq. (3.7) becomes an algebraic function

$$\left\langle \prod_{j=1}^n e^{i\kappa_j \phi(x_j)} \right\rangle = F(\Lambda) \prod_{\substack{i,j \\ i \neq j}} (|x_i - x_j|)^{\kappa_i \kappa_j / 2\pi}. \quad (3.13)$$

Let us make two remarks on this expression:

1. We are interested in the limit $m \rightarrow 0$. This puts a constraint on the coefficients κ_i : $\sum \kappa_i$ must vanish in order to cancel the $\log m$ term in eq. (3.12).
2. From eq. (3.12), it is clear that the UV cutoff Λ introduces a factor of the form

$$F(\Lambda) = \prod_j \Lambda^{\frac{\kappa_j^2}{2\pi}}.$$

It can be removed by a multiplicative renormalization of $e^{i\kappa_j\phi} \rightarrow \zeta_j e^{i\kappa_j\phi}$ with a renormalization constant $\zeta_j = (\Lambda/\mu)^{-\frac{\kappa_j^2}{4\pi}}$. This cancels $F(\Lambda)$ and rescales the expression in eq. (3.13) by the renormalization scale μ . So for simplicity, we can think of it as a relation among renormalized fields.

Finally, we want to consider the particular case where the κ_i take the two values $\pm\kappa$ only. Note that the constraint for taking the limit $m \rightarrow 0$ is met, if we have an equal number of κ and $-\kappa$. In this case, we can evaluate the expectation value in the massless limit and get

$$\left\langle \prod_{i=1}^n e^{i\kappa(\phi(x_i) - \phi(z_i))} \right\rangle \propto \frac{\prod_{i<j} |x_i - x_j|^{\frac{\kappa^2}{2\pi}} |z_i - z_j|^{\frac{\kappa^2}{2\pi}}}{\prod_{ij} |x_i - z_j|^{\frac{\kappa^2}{2\pi}}}. \quad (3.14)$$

If we set $\kappa = 4\pi$, the rhs is indeed equal to the correlators of the fermionic σ_{\pm} operators in eq. (3.6), up to numerical factors. This is the promised correspondence between fermionic and bosonic correlation functions. It can formally be expressed as an operator identity by setting

$$2\pi\sigma_+ = \Lambda e^{i\sqrt{4\pi}\phi(x)} \quad \text{and} \quad 2\pi\sigma_- = \Lambda e^{-i\sqrt{4\pi}\phi(x)}. \quad (3.15)$$

Evidently, if we replace the operators, we also have to evaluate functional integrals in the other theory.

3.3 The Free Massive Fermion

As an intermediate step on our way to the bosonized Schwinger model, we apply the analogy derived above to a massive free fermion. We start with the partition function

$$\mathcal{Z} = \int D\bar{\psi} D\psi e^{-S_F^m} \quad (3.16)$$

taken with the massive fermion action

$$S_F^m[\bar{\psi}, \psi] = \int d^2x \left[\bar{\psi}(x) \not{\partial} \psi(x) + m \bar{\psi}(x) \psi(x) \right]. \quad (3.17)$$

We still think of the quark fields as γ_5 eigenstates. The mass term can be written as $m\sigma_+ + m\sigma_-$, acting as a source for the σ fields. Suppose m is small, then, we can turn the mass term into a series of n-point functions of the σ_{\pm} fields by expanding the exponential. Those are evaluated with the massless action (3.1):

$$\int D\bar{\psi} D\psi e^{-S_F^m} = \sum_n \frac{1}{n!} \left\langle \left[\int d^2x m\sigma_+ + m\sigma_- \right]^n \right\rangle_{S^F (m=0)}. \quad (3.18)$$

At this point, we make use of the operator relation in eq. (3.15) and express the σ_{\pm} operators through their scalar equivalents. Note, that at the same time we switch to taking the expectation values with respect to the action of the *massless scalar* in eq. (3.8). Thus, eq. (3.18) becomes

$$\sum_n \frac{1}{n!} \left(\frac{\Lambda}{2\pi} \right)^n \left\langle \left[\int d^2x m e^{i\sqrt{4\pi}\phi(x)} + m e^{-i\sqrt{4\pi}\phi(x)} \right]^n \right\rangle_{S^S(m=0)}. \quad (3.19)$$

We sum this expression in the bosonic theory and obtain the partition function of a theory with the action

$$S^{SG}[\phi] = \int d^2x \left[\frac{1}{2} (\partial_{\mu}\phi(x))^2 + \frac{\Lambda}{2\pi} (m e^{i\sqrt{4\pi}\phi(x)} + m e^{-i\sqrt{4\pi}\phi(x)}) \right]. \quad (3.20)$$

This is the action of a massless Sine Gordon model. Thus, the partition function of a free massive fermion is equivalent to the one of a particular Sine Gordon model with $\alpha = m\Lambda/\pi$

$$\mathcal{Z}^{SG} = \int D\phi \exp \left(- \int d^2x \left[\frac{1}{2} (\partial_{\mu}\phi)^2 + \alpha \cos(\sqrt{4\pi}\phi) \right] \right). \quad (3.21)$$

3.4 Bosonizing the Schwinger Model

Let us return to the Schwinger model and apply the results of the last three sections to it. As we have promised, it will be possible to see from the bosonized theory what particles the model contains. Also, the exact solution of the massless model is obtained through this technique [14]. However, here we will directly head for the bosonized version of the model with two degenerate, massive fermion flavors, which interests us most.

Once more we do a local chiral transformation on the quark fields

$$\psi^a(x) \rightarrow \psi'^a(x) = e^{\gamma_5 \zeta(x)} \psi^a(x) \quad \bar{\psi}^a(x) \rightarrow \bar{\psi}'^a(x) = \bar{\psi}^a(x) e^{\gamma_5 \zeta(x)}, \quad (3.22)$$

$a = 1, 2$ is a flavor index. The flavor components do not mix under this change of variables. They are both modified by the same field $\zeta(x)$. We discussed a similar transformation, with an imaginary parameter $i\alpha(x)$, already in the chapters on chiral symmetry and the axial anomaly, 2.3.2 and 2.3.3 respectively. We will recall some of the properties derived there and see how they can be related to the bosonization technique. We remark that the transformation in eq. (3.22) is not unitary, which however does not matter here, since we are not interested in symmetries of the action of the Schwinger model, but rather are about to transform it into a different theory.

The manipulation has essentially three effects:

1. For each flavor component it generates a term

$$\bar{\psi}^a(x) \gamma^\mu [\partial_\mu \gamma_5 \zeta(x)] \psi^a(x) = i \bar{\psi}^a(x) \epsilon_{\mu\nu} \gamma^\nu [\partial^\mu \zeta(x)] \psi^a(x)$$

in the action. This term is proportional to the one which became the divergence of the axial current in section 2.3.2. Here, we made use of the two dimensional relation in eq. (2.20) and traded the axial for the vector current. After this, the fermionic sector of the action is

$$\int d^2x \left[\sum_a \bar{\psi}^a \not{\partial} \psi^a + i g_0 A_\mu J_\mu + i \epsilon_{\mu\nu} J_\nu (\partial_\mu \zeta) \right]. \quad (3.23)$$

If we set $A_\nu(x) = -g_0^{-1} \epsilon_{\mu\nu} \partial_\mu \zeta(x)$ the last two terms cancel and the covariant derivative reduces to a simple one.

2. The transformation eq. (3.22) is anomalous. As we saw in section 2.3.3, a infinitesimal rotation of this kind generates the non trivial Jacobian (2.41) in the partition function. But $\zeta(x)$ is not necessarily small, so in order to investigate the anomaly term in the present case, we must construct ζ from a sequence of infinitesimal rotations. To this end we introduce a parameter $\alpha \in [0, 1]$ and rescale $\zeta(x) \rightarrow \alpha \zeta(x)$; $\delta\alpha \zeta(x)$ is then infinitesimal as required. We define $\Gamma(\delta\alpha) \equiv \log \det \mathcal{J}^2(\delta\alpha)$. In eq. (2.35) we saw that $\Gamma(i\delta\alpha) = 2i \delta\alpha \zeta \text{ tr } T$, with the matrix T as it was defined in eq. (2.36). Thus, we can write here

$$\Gamma(\delta\alpha) = 2(\alpha + \delta\alpha) \zeta \text{ tr } T - 2\alpha \zeta \text{ tr } T = \Gamma(\alpha + \delta\alpha) - \Gamma(\alpha). \quad (3.24)$$

The above expression is valid up to $O(\delta\alpha^2)$ and we can write it as

$$\frac{\partial\Gamma(\alpha)}{\partial\alpha} = 2 \zeta \text{ tr } \mathbb{T} = \frac{g_0}{2\pi} \int d^2x \zeta(x) \epsilon_{\mu\nu} F_{\mu\nu}(x) = -\frac{\alpha}{\pi} \int d^2x \zeta(x) \partial^2 \zeta(x). \quad (3.25)$$

In the last step we expressed the field strength tensor $F_{\mu\nu}$ by the particular gauge field we have chosen above (where ζ appearing in A_μ was rescaled to $\alpha\zeta$)

$$F_{\mu\nu}(x) = -\frac{\alpha}{g_0} \epsilon_{\mu\nu} \partial^2 \zeta(x).$$

Integrating over α in eq. (3.25) yields the full transformation with macroscopic $\zeta(x)$, hence

$$\Gamma(1) - \Gamma(0) = \log \det \mathcal{J}^2 = -\frac{1}{2\pi} \int d^2x \zeta(x) \partial^2 \zeta(x)$$

Since we have two flavors, the Jacobian appears once for the transformation of each of them. So finally, the change of the fermion fields in eq. (3.22) generates an additional factor of

$$\mathcal{J}^4 = e^{-\frac{1}{\pi} \int d^2x \zeta \partial^2 \zeta}.$$

3. The mass term transforms as

$$m_0 \bar{\psi}^a \psi^a \rightarrow m_0 \bar{\psi}^a e^{2\gamma_5 \zeta} \psi^a.$$

If we write ψ^a and $\bar{\psi}^a$ as γ_5 eigenstates, it separates into two terms, one with σ_- and one with σ_+

$$\begin{aligned} \bar{\psi}^a m_0 e^{2\zeta \gamma_5} \psi^a &= m_0 e^{2\zeta} \sigma_+^a + m_0 e^{-2\zeta} \sigma_-^a \\ &= \frac{m_0 \Lambda}{2\pi} (e^{i(\sqrt{4\pi}\phi^a - 2i\zeta)} + e^{-i(\sqrt{4\pi}\phi^a - 2i\zeta)}). \end{aligned} \quad (3.26)$$

In the second step we made use of the operator relation in eq. (3.15) and expressed the σ_\pm operators through boson fields. We have to introduce two fields ϕ^1 and ϕ^2 , one for each flavor component.

The fermion sector of the action is therefore formally equivalent to the one of a massive free fermion and can be bosonized by the argument given in section 3.3. The only difference being that there are contributions of the ζ field in the argument of the cosine. There remain the contributions from the gauge action and the anomaly. They can both be formulated in terms of ζ .

Putting all terms together, the two flavor Schwinger model is equivalent to a bosonic theory with the action

$$S[\phi_1, \phi_2, \zeta] = \int d^2x \left[\frac{1}{2}(\partial_\mu \phi_1)^2 + \frac{1}{2}(\partial_\mu \phi_2)^2 + \frac{m_0 \Lambda}{\pi} \left(\cos(\sqrt{4\pi} \phi_1 - 2i\zeta) + \cos(\sqrt{4\pi} \phi_2 - 2i\zeta) \right) - \frac{1}{\pi} \zeta \partial^2 \zeta + \frac{1}{2g_0^2} (\partial^2 \zeta)^2 \right]. \quad (3.27)$$

The very last term comes from the gauge action, the second last from the anomaly.

The action (3.27) can be simplified further by shifting ϕ_a to $\phi_a + \frac{i}{\sqrt{\pi}} \zeta$. Therewith, the ζ contribution in the cosine and the term $\pi^{-1} \zeta \partial^2 \zeta$ cancel and we can write eq. (3.27) as

$$S[\phi_1, \phi_2, \zeta] = \int d^2x \left[\sum_{a=1}^2 \frac{1}{2} (\partial_\mu \phi_a)^2 + \frac{m_0 \Lambda}{\pi} \cos(\sqrt{4\pi} \phi_a) + \frac{i}{2\sqrt{\pi}} (\partial_\mu \zeta \partial_\mu \phi_a + \partial_\mu \phi_a \partial_\mu \zeta) + \frac{1}{2g_0^2} (\partial^2 \zeta)^2 \right]. \quad (3.28)$$

The partition function is now Gaussian in $g_0^{-1} \zeta$ and it can be integrated out. The coupling to the ϕ_a fields introduces a mass term for $\phi_1 + \phi_2$. We reformulate eq. (3.28) in terms of $\phi_\pm = \frac{1}{\sqrt{2}}(\phi_1 \pm \phi_2)$ and finally obtain

$$S[\phi_+, \phi_-] = \int d^2x \left[\frac{1}{2} (\partial_\mu \phi_+)^2 + \frac{1}{2} (\partial_\mu \phi_-)^2 + \frac{g_0^2}{\pi} \phi_+^2 + \frac{2m_0 \Lambda}{\pi} \cos(\sqrt{2\pi} \phi_+) \cos(\sqrt{2\pi} \phi_-) \right]. \quad (3.29)$$

Hence, the massive two flavor Schwinger model contains two scalar particles, one of them, the ϕ_- , is massless in the limit of vanishing quark mass, the other retains a finite mass $\mu = \sqrt{2g_0^2/\pi}$ even in the chiral limit. A finite fermion mass m_0 introduces interactions in the form of cosines of the fields, the model is then no longer exactly solvable. The bosonized action eq. (3.29) hides the flavor symmetry of the theory. Nevertheless, one can show [15] that ϕ_+ can be constructed from isosinglet operators of the fermionic theory. It gets its mass mainly through the axial anomaly. Therefore, it is often referred to as the η particle of the Schwinger model. The ϕ_- field has complicated transformation properties. However, all three isospin non-singlet vector currents of table 2.2 can be written as functions of ϕ_- . It thus propagates a degenerate isospin

triplet, which is called the pion π . We will stick to the common usage and call the two particles π and η in later chapters.

There exist several approximate solutions of the model in the limit of $m_0 \ll g_0$, i.e. $m_0 \ll \mu$. There, the η particle is expected to become so heavy that it freezes out, i.e. $\phi_+(x) \equiv 0$. The action in eq. (3.29) reduces then to the one of the Sine-Gordon model which can be solved exactly [16] or by semi-classical methods.

In these solutions, one obtains the relation

$$m_{gap} = A_g m_0^{2/3} g_0^{1/3} \quad (3.30)$$

for the dependence of the mass gap on the quark mass. The constant A_g depends on how the approximation is evaluated in detail. Smilga [17] gives three values for A_g

$$A_g = \begin{cases} 2.008.. & \text{exact solution for } \phi_+ = 0 \text{ in eq. (3.29)} \\ 2.07.. & \text{semi-classical, with } m_{gap} = \text{soliton mass} \\ 2.1633.. & \text{semi-classical, with } m_{gap} = \text{classical Sine Gordon mass.} \end{cases} \quad (3.31)$$

We will use these values later to compare them with our results.

Chapter 4

The Schwinger Model on the Lattice

In the last two chapters we studied the Schwinger model in the continuum. Here, we introduce the theory regularized on the lattice and discuss the theoretical argument which we exposed in the introduction in more detail.

4.1 Formulation of the Lattice Theory

We want to formulate the Schwinger model on a finite isotropic space time lattice with lattice spacing a , and volume $(L \times T)$. Instead of continuous space time variables x , we have a set of discrete points $x = (na)$ where n is a vector of two integer values in the range $(0, \frac{L}{a}]$ and $(0, \frac{T}{a}]$ respectively. We denote the unit vector of length a in the μ - direction by $\hat{\mu}$.

In Fourier space, functions defined on the lattice are periodic with a period $\frac{2\pi}{a}$. Therefore, we can restrict ourselves to the first Brillouin zone $p \in (-\pi/a, \pi/a]$. The lattice acts as a momentum cutoff at $p_{max} = \frac{\pi}{a}$. Sending the cutoff to infinity corresponds to taking the continuum limit $a \rightarrow 0$. In addition, in finite volume the momenta become discrete and are quantized in steps of $\frac{2\pi}{L}$ or $\frac{2\pi}{T}$.

4.1.1 Fields on the Lattice

The lattice fermion fields $\bar{\psi}$ and ψ are anticommuting Grassmann variables supported on the lattice sites only. The formulation of the gauge field is less straightforward. In the continuum, a particle travelling on a path C through

an Abelian gauge field A_μ , picks up a phase

$$\psi'(x) = \exp(ig_0 \int_C A_\mu(z) dz_\mu) \psi(x).$$

Accordingly, taking A_μ to be constant over a displacement of a , a fermion field hopping to a neighboring lattice site is given by

$$\psi_{na+\hat{\mu}}(na) \equiv \psi'(na) = e^{iag_0 A_\mu(na)} \psi(na).$$

The gauge field can thus be formulated in terms of parallel transporters $U_\mu(x) = e^{iag_0 A_\mu(x)}$ living on the links between two adjacent lattice sites [18]. It follows immediately that

$$U_{-\mu}(x) = e^{-iag_0 A_\mu(x-\hat{\mu})} = U_\mu^\dagger(x - \hat{\mu}).$$

Note, that in this formulation the gauge fields become compact variables while the field A_μ ranges over the entire real axis.

Under a gauge transformation $V(x)$ the fermion fields transform as in the continuum

$$\psi(x) \rightarrow V(x)\psi(x) \qquad \bar{\psi}(x) \rightarrow \bar{\psi}(x)V^\dagger(x),$$

where $V(x)$ is a local phase factor. The gauge fields however transform as

$$U_\mu(x) \rightarrow V(x)U_\mu(x)V^\dagger(x + \hat{\mu}).$$

It is easy to see that any gauge invariant quantity on the lattice is either a closed chain of link variables, a so called Wilson loop, or a string of oriented link variables sandwiched between a $\psi - \bar{\psi}$ pair. On a lattice with periodic boundary conditions, the fermions can be omitted if the string extends over the whole lattice, this is then called a Polyakov line.

4.1.2 Wilson Gauge Action

Once we know how to express the fields on the lattice, we have to discretize the action. There are various ways to do this, the only requirement being that in the limit $a \rightarrow 0$ one retrieves the continuum theory. In addition, one should try to maintain as many symmetries of the continuum action as possible. This is not a trivial statement, as can be seen from the fact that the lattice does not even have the full Poincaré group. It is invariant only under rotations of an angle of $\pi/2$ (in the case of $T = L$) and translations by multiples of a . The last statement is equivalent to the fact that there are only

discrete momenta $k_n = \frac{2\pi an}{L}$. Much more serious effects arise however, from the breaking of internal symmetries by the lattice action as will be discussed below.

In 1974 Wilson proposed

$$S_G[U] = \beta \sum_x \sum_{\mu < \nu} \text{Re tr} (1 - W_{\mu\nu}(x)) \quad (4.1)$$

as the lattice equivalent of the gauge action $F_{\mu\nu}F^{\mu\nu}$ [18]. Here, $W_{\mu\nu}$ is the plaquette

$$W_{\mu\nu}(x) = U_\mu(x)U_\nu(x + \hat{\mu})U_\mu^\dagger(x + \hat{\nu})U_\nu^\dagger(x) = W_{\nu\mu}^\dagger(x) \quad (4.2)$$

and β the dimensionless gauge coupling $\beta = \frac{1}{a^2 g_0^2}$. In two dimensions, the sum over $\mu < \nu$ can be omitted; also for the gauge group $U(1)$ we can skip the trace. Eq. (4.1) reduces to the continuum gauge action up to discretization errors of $O(a)$. This is particularly easy to show in the Abelian case. Since the gauge fields A_μ commute, we can write the plaquette as

$$\begin{aligned} W_{\mu\nu}(x) &= e^{ia g_0 (A_\mu(x) + A_\nu(x + \hat{\mu}) - A_\mu(x + \hat{\nu}) - A_\nu(x))} = e^{ia^2 g_0 (\partial_\nu A_\mu(x) - \partial_\mu A_\nu(x)) + O(a^3)} \approx \\ &\approx 1 - \frac{a^4 g_0^2}{2} F_{\mu\nu}^2(x) + O(a^5) + i(a^2 g_0 F_{\mu\nu}(x) + O(a^3)). \end{aligned} \quad (4.3)$$

Inserting this expansion into eq. (4.1) we get

$$S_G[U] = \frac{a^2}{4} \sum_x \left(\sum_{\mu, \nu} F_{\mu\nu}^2(x) + O(a) \right).$$

The additional factor of $\frac{1}{2}$ arises because of the summation over μ and ν . In the limit $a \rightarrow 0$, $a^2 \sum_x$ becomes the integral $\int d^2x$ and the higher order terms in a vanish.

4.1.3 Confinement

At this point, we return to the question of confinement which we left open in the 2. chapter. In order to investigate it, one has to look at the potential $V(R)$ between a static quark-antiquark pair $q\bar{q}$ separated by a distance R . If the potential increases with growing R , the quarks are confined. We think of a $q\bar{q}$ pair kept apart at a fixed spatial distance R , travelling through time from t to $t + T$. It propagates on a closed path C through spacetime. On its way, it picks up a phase determined by the transition amplitude

$$\mathcal{W}(C) = \langle e^{ig_0 \oint_C A_\mu(z) dz_\mu} \rangle = \langle J(x + T) | e^{-HT} | J(x) \rangle,$$

where $J(x) = \bar{q}(x_0, \mathbf{x}) \prod_{i=\mathbf{x}}^{\mathbf{y}-1} U_1(x_0, i) q(x_0, \mathbf{y})$ denotes the pair and $R = |\mathbf{x} - \mathbf{y}|$. Thus, $V(R)$ can be defined as

$$V(R) = - \lim_{T \rightarrow \infty} \frac{1}{T} \log \mathcal{W}(C).$$

We also define the string tension σ [8] by

$$\sigma \equiv \lim_{R \rightarrow \infty} \frac{1}{R} V(R).$$

For instance, in the case of a linearly rising potential i.e. $V(R) \propto R$, σ is constant and the transition amplitude $\mathcal{W}(C)$ is proportional to $e^{-\sigma RT}$. This is the so called area law. The perimeter law, on the other hand, where $\mathcal{W} \propto e^{-\alpha(R+T)}$, does not signal confinement, the string tension vanishes.

On the lattice, the potential $V(R)$ can be measured by the expectation value of Wilson loops, which are the trace of the parallel transporters around a closed path on the lattice. In our Abelian model, they simply become the product of the link variables along that path

$$\mathcal{W}(C) = \prod_{x \in C} U_\mu(x). \quad (4.4)$$

The Schwinger model is confining at any gauge coupling [10]. This is a general property of a $U(1)$ gauge theory in two dimensions, the argument can thus be made in pure gauge, neglecting the fermionic action.

In order to derive confinement, we choose a rectangular $l \times t$ Wilson loop. The product \mathcal{W} in eq. (4.4) is equivalent to the product of all plaquettes on the surface enclosed by C . The gauge links in the interior of the area cancel, because they appear twice in two neighboring plaquettes, once as $U_\mu(x)$ and once as $U_\mu^\dagger(x)$. The expectation value of \mathcal{W} can thus be written as

$$\langle \mathcal{W} \rangle = \frac{1}{\mathcal{Z}} \int \prod_{x,\mu} dU_\mu(x) \prod_{x \in \mathcal{W}} W_{01}(x) e^{-S_G[U]}, \quad (4.5)$$

where $S_G[U]$ is the Wilson plaquette action and W_{01} is the plaquette itself. We choose a temporal gauge, setting all U_0 to 1, and free boundary conditions, then $\langle \mathcal{W} \rangle$ becomes

$$\begin{aligned} \langle \mathcal{W} \rangle &= \\ &= \frac{1}{\mathcal{Z}} \int \prod_x dU_1 \left(\prod_{x \in \mathcal{W}} \text{Re} U_1(x) U_1^\dagger(x + \hat{0}) e^{-\beta \text{Re}[1 - U_1(x) U_1^\dagger(x + \hat{0})]} \right) \\ &\quad \left(\prod_{x \notin \mathcal{W}} e^{-\beta \text{Re}[1 - U_1(x) U_1^\dagger(x + \hat{0})]} \right). \end{aligned} \quad (4.6)$$

The second parenthesis cancels with the corresponding factors in \mathcal{Z} . The other terms are $l \times t$ equivalent integrals. In eq. (4.6), we write explicitly $\text{Re } U_1(x)U_1^\dagger(x + \hat{0})$ to make the following step clearer, in the gauge average $\langle \mathcal{W} \rangle$ is real anyway due to charge conjugation. We imagine doing a gauge transformation such that $U_1'(x) \leftarrow U_1(x)U_1^\dagger(x + \hat{0})$, then eq. (4.5) becomes

$$\langle \mathcal{W} \rangle = \left(\frac{\partial_\beta \tilde{\mathcal{Z}}}{\tilde{\mathcal{Z}}} \right)^{lt}, \quad (4.7)$$

where $\tilde{\mathcal{Z}} = \int dU_1 e^{\beta \text{Re} U_1}$. $\langle \mathcal{W} \rangle$ shows a clear area law. The potential rises linearly with l irrespective of the value of β . Our two dimensional model has therefore only a confining phase.

The introduction of fermions in the action results in a redefinition of $\tilde{\mathcal{Z}}$ which has to include the fermion matrix of eq. (5.1).

4.1.4 Fermions on the Lattice

Naïve Fermion Action and Fermion Doubling

The most straightforward way to formulate the fermion action on the lattice is to replace the derivative operator by a symmetrized covariant difference operator

$$\begin{aligned} \bar{\psi} \not{D}_c \psi &\rightarrow \frac{1}{2a} \sum_\mu \bar{\psi}(x) \gamma_\mu [U_\mu(x) \psi(x + \hat{\mu}) - U_\mu^\dagger(x - \hat{\mu}) \psi(x - \hat{\mu})] \\ &= \bar{\psi}(x) \left[\frac{1}{2} \sum_{\mu=0}^1 \gamma^\mu (\nabla_\mu^* + \nabla_\mu) \right] \psi(x) = \bar{\psi}(x) \not{D}_{lat}(x, y) \psi(y), \end{aligned} \quad (4.8)$$

where in the second step we introduced the lattice forward and backward derivatives

$$\begin{aligned} \nabla_\mu \psi(x) &= \frac{1}{a} (U_\mu(x) \psi(x + \hat{\mu}) - \psi(x)) \\ \nabla_\mu^* \psi(x) &= \frac{1}{a} (\psi(x) - U_\mu^\dagger(x - \hat{\mu}) \psi(x - a\hat{\mu})). \end{aligned} \quad (4.9)$$

The parallel transporters are included to maintain gauge invariance. The correct continuum covariant derivative \not{D}_c is obtained from this expression up to $O(a^2)$ by expanding the exponentials U_μ and writing $\psi(x \pm \hat{\mu})$ as a Taylor series.

However, this so called naïve fermion action does not produce the desired continuum theory. To see this, we investigate the free theory, setting $U_\mu = 1$. The propagator of a massless free naïve fermion S_F is determined by

$$\begin{aligned} \mathbb{D}_{lat}(x, y) S_F(y, z) &= \delta(x, z) = \int_{-\pi/a}^{\pi/a} \frac{d^d p}{(2\pi)^d} e^{ip(x-z)} = \int_{-\pi/a}^{\pi/a} \frac{d^d p}{(2\pi)^d} \mathbb{D}_{lat} e^{ip(x-z)} S_F(p) \\ &= \int_{-\pi/a}^{\pi/a} \frac{d^d p}{(2\pi)^d} \frac{1}{2a} \sum_{\mu} \gamma_{\mu} (e^{ip\hat{\mu}} - e^{-ip\hat{\mu}}) e^{ip(x-z)} S_F(p), \end{aligned} \quad (4.10)$$

from which we conclude that $S_F^{-1}(p) = \frac{i}{a} \sum_{\mu} \gamma_{\mu} \sin(ap_{\mu})$. For small momentum p , we can expand the sine function and get the continuum propagator up to $O(a^2)$ effects. Unfortunately, due to the periodicity of the sine, S_F^{-1} vanishes not only in the center of the Brillouin zone at $p = (0, 0)$, but also at its edges, where $p_{\mu} = \frac{\pi}{a}$. Instead of one, we have 2^d fermions. This is the so called fermion doubling problem [19]. The introduction of interactions does not mend this defect. The appearance of the doublers is related to the problem of chiral symmetry on the lattice by the Nielsen Ninomiya theorem [20].

One possibility to avoid doubling was again proposed by Wilson [21], he added a term of higher dimension, the so called Wilson term $\frac{ra}{2} \bar{\psi} \partial^2 \psi$, to the continuum action. Here, r is a parameter ranging from 0 to 1. We use $r = 1$ in this work. With ∇ and ∇^* as given in eq. (4.9), the lattice action of massless Wilson fermions in d dimensions is given by

$$\begin{aligned} S_W &= a^d \sum \bar{\psi}(x) \left[\frac{1}{2} \sum_{\mu=0}^1 (\gamma^{\mu} (\nabla_{\mu}^* + \nabla_{\mu}) - ar \nabla_{\mu}^* \nabla_{\mu}) \right] \psi(x) = \\ &= a^d \sum_x \bar{\psi}(x) D_W \psi(y), \end{aligned} \quad (4.11)$$

where we defined the Wilson operator D_W by

$$D_W = \frac{1}{2} \sum_y [\gamma^{\mu} (\nabla_{\mu}^* + \nabla_{\mu}) - ar \nabla_{\mu}^* \nabla_{\mu}]. \quad (4.12)$$

The Wilson term vanishes in the naïve continuum limit. For the case of free fermions, the propagator at finite lattice spacing is modified to

$$S_F^{-1}(p) = \sum_{\mu} \left[\frac{i}{a} \gamma_{\mu} \sin(ap_{\mu}) + \frac{r}{a} (1 - \cos(p_{\mu}a)) \right]. \quad (4.13)$$

The cosine term vanishes at $p_\mu = 0$, but remains finite at $p_\mu = \frac{\pi}{a}$ giving a mass proportional to $\frac{1}{a}$ to the doublers. In the limit $a \rightarrow 0$, they become infinitely heavy and move away from the physical spectrum.

The Wilson action S_W is very often given in terms of the hopping parameter κ , which in d dimension is equal to

$$\kappa = \frac{1}{2am_0 + 2dr}. \quad (4.14)$$

The action itself

$$S_W = \sum_x \bar{\psi}(x) [\psi(x) - \kappa \sum_\mu [r - \gamma^\mu] U_\mu(x) \psi(x + a\hat{\mu}) + [r + \gamma^\mu] U_\mu^\dagger(x - a\hat{\mu}) \psi(x - a\hat{\mu})] \quad (4.15)$$

is obtained from eq. (4.12) by rescaling the fermions (in 2 dimensions) from ψ to $a^{1/2}(am_0 + 2r)^{\frac{1}{2}}\psi$. Also, we have unadmittedly sneaked in a mass term $m_0\bar{\psi}\psi$ in eq. (4.12). It is this form of S_W that we implemented in the simulations. The Wilson term has a piece which is proportional to the mass term. Therefore, it may lead to an additive correction of the quark mass and one writes

$$m_q = m_0 - m_{cr}. \quad (4.16)$$

m_q is called the bare subtracted quark mass. The critical mass m_{cr} is defined as the value of m_0 , where the physical quark mass vanishes. In the interactive theory m_{cr} depends on the size of the cutoff, such that the quark mass needs both additive and multiplicative renormalization. But most importantly, chiral symmetry is explicitly broken by the Wilson term. If we were to derive the PCAC relation for Wilson fermions as in section 2.3.5, an additional piece resulting from the Wilson term would appear in δS [22]. This term is proportional to ra and mixes with chirally non invariant operators. Thus, even in the limit of vanishing quark mass chiral symmetry is violated at $O(a)$.

4.2 Cutoff Effects

The lattice action is equivalent to the continuum one only up to terms of higher order in the lattice spacing a . These terms become irrelevant in the limit $a \rightarrow 0$. However, at finite a their presence modifies the physical quantities extracted from the theory by so called cutoff effects.

A systematic description of cutoff effects was proposed by Symanzik [1]. He introduced a continuum Lagrangian which mimics the lattice Lagrangian

at finite a . There, the lattice spacing appears as an effective coupling associated with operators of dimension larger than d . These can be imagined as arising from integrating out the momenta in the range $(\frac{\pi}{a}, \infty)$ in the continuum action. In this sense, the lattice action is replaced by an effective low energy continuum theory with

$$S_{\text{eff}} = \int d^d x (\mathcal{L}_0(x) + a\mathcal{L}_1(x) + a^2\mathcal{L}_2(x) + O(a^3)), \quad (4.17)$$

where \mathcal{L}_0 is the Lagrangian of the limiting continuum theory and \mathcal{L}_j contains all operators of dimension $d + j$ allowed by the symmetries of the lattice theory. To first order in a , the Wilson action is modified by the so called Sheikholeslami-Wohlert- or clover term

$$S_W \rightarrow S_W + a^{d+1} \sum_x c_{sw} \bar{\psi}(x) \frac{i}{4} \sigma_{\mu\nu} F_{\mu\nu} \psi(x). \quad (4.18)$$

This term is not chirally invariant and appears in \mathcal{L}_1 because chiral symmetry is not preserved by the Wilson action. Since we are interested in on-shell improvement other dimension $d+1$ terms can be eliminated by the equations of motion and in a massless renormalization scheme, the remaining terms in \mathcal{L}_1 result in a rescaling of the bare mass and the coupling constant [3]

$$\begin{aligned} g_0 &\rightarrow g_0(1 + ab_g m_q) \\ m_q &\rightarrow m_q(1 + ab_m m_q). \end{aligned} \quad (4.19)$$

The same considerations apply to local composite fields which we can write as

$$\phi_{\text{eff}}(x) = \phi_0(x) + a\phi_1(x) + a^2\phi_2(x) + O(a^3). \quad (4.20)$$

The ϕ_j contain all operators of dimension $[\phi_0] + j$, which transform in the same way as the lattice operator in question. The expectation value of ϕ_{eff} in the effective theory becomes

$$\langle \phi_{\text{eff}} \rangle = \langle \phi_0 \rangle_0 + a \langle \int d^d x \phi_0 \mathcal{L}_1 \rangle_0 + a \langle \phi_1 \rangle_0 + O(a^2). \quad (4.21)$$

The subscript 0 indicates here that the expectation value is taken with respect to the limiting continuum action, i.e. $\int \mathcal{L}_0 d^d x$, only.

¹Note that for $d = 2$ this formulation of the clover term has the correct mass dimension only, if we rescale the gauge field $A_\mu \rightarrow g_0 A_\mu$, (assuming c_{sw} to be dimensionless). This modifies the continuum Lagrangian of the Schwinger model to $\bar{\psi}[\not{\partial} + i\gamma^\mu A_\mu + m_0]\psi + \frac{1}{4g_0^2} F^{\mu\nu} F_{\mu\nu}$. The derivation of the lattice action and fields remains unchanged.

Numerical simulations are always done at finite a . To extract continuum values, one has to simulate at different lattice spacings and extrapolate the results to $a = 0$. In order to make this extrapolation reliable, one has to know how the continuum is approached as a function of the lattice spacing. If we think of the lattice action as a power series in a as in eq. (4.17), then the higher the leading order of the cutoff effects, the smoother the extrapolation. That is at higher order the size of the lattice artifacts decreases more rapidly with smaller a and the extrapolation is effectively over a shorter lever.

Different discretizations of the continuum theory differ by the form of their cutoff effects. It is highly profitable to choose an action where they are as small as possible at a reasonable computational cost. In the case of Wilson fermions in QCD in large volume, the Wilson term introduces cutoff effects linear in a which happen to be rather large [3]. Consequently a lot of effort has been made to improve the Wilson action by one order, adding a counter term and tuning its coefficient c_{sw} such that the $O(a)$ effects cancel.² This attempt to get rid of cutoff effects order by order is known as the Symanzik improvement programme [1]. The link between chiral symmetry and $O(a)$ lattice artifacts can be understood from the fact that the correct tuning of the coefficients can be reached by imposing chiral symmetry restoration up to $O(a^2)$ [23].

4.2.1 Cutoff Effects and Spontaneous Chiral Symmetry Breaking

In this section we introduce a so called “spurionic” symmetry of the Wilson lattice action. We will see that multiplicatively renormalizable operators can be classified into even or odd operators under this transformation. Such an analysis was first presented in ref. [2]. It proved to be helpful to further investigate the nature of lattice artifacts for Wilson fermions. We will argue that the appearance of large cutoff effects linear in the lattice spacing in QCD is tied not only to the explicit breaking of chiral symmetry by the Wilson term, but also to the fact that chiral symmetry is spontaneously broken.

The Spurionic Symmetry

Consider the transformation

$$R^5 = \begin{cases} \psi \rightarrow \gamma_5 \psi \\ \bar{\psi} \rightarrow -\bar{\psi} \gamma_5. \end{cases} \quad (4.22)$$

²Naturally, at the same time the local field operators have to be improved in analogous way.

R^5 can be written as the product of two isovector and one axial isovector transformations: $u_V^1(\pi) = e^{i\pi\frac{\tau_1}{2}}$, $u_V^2(\pi) = e^{i\pi\frac{\tau_2}{2}}$ and $u_A^3(\pi) = e^{i\pi\gamma_5\frac{\tau_3}{2}}$ with

$$u_V^1(\pi) = \cos \frac{\pi}{2} + i\tau_1 \sin \frac{\pi}{2} = i\tau_1. \quad (4.23)$$

Similarly, we have $u_V^2(\pi) = i\tau_2$ and $u_A^3(\pi) = i\gamma_5\tau_3$. Hence, R^5 acts on ψ as

$$\begin{aligned} u_V^1(\pi) u_V^2(\pi) u_A^3(\pi) \psi &= -i\tau_1\tau_2\tau_3\gamma_5 \psi = -\frac{i}{2}(\tau_1\tau_2 - \tau_2\tau_1) \tau_3\gamma_5 \psi = \\ &= \tau_3^2\gamma_5 \psi = \gamma_5 \psi. \end{aligned} \quad (4.24)$$

In the same way, we get for the adjoint spinor $\bar{\psi}$

$$\bar{\psi} u_A^3(\pi) u_V^{2\dagger}(\pi) u_V^{1\dagger}(\pi) = -i\bar{\psi} \gamma_5\tau_3\tau_2\tau_1 = i\bar{\psi} \gamma_5\tau_3\tau_1\tau_2 = -\bar{\psi} \gamma_5. \quad (4.25)$$

Thus, R^5 is a sound, non anomalous transformation for any theory with a $SU(2)_L \times SU(2)_R$ flavor symmetry. If we transform the quark fields in the Wilson fermion action by R^5 , the kinetic term is invariant, whereas the Wilson and the mass term change sign. Hence, S_W is invariant under the spurionic transformation

$$R_{sp}^5 = R^5 \times [r \rightarrow -r] \times [m_0 \rightarrow -m_0], \quad (4.26)$$

where we change the sign of the Wilson- and the mass term simultaneously with R^5 . The so defined symmetry not only acts on the fields but also transforms external parameters, relating in this sense different regularizations. R_{sp}^5 can also be given in terms of the subtracted quark mass m_q

$$R_{sp}^5 = R^5 \times [r \rightarrow -r] \times [m_q \rightarrow -m_q]. \quad (4.27)$$

Eqs. (4.27) and (4.26) are equivalent, if the critical mass $m_{cr}(r, \beta)$ is odd as a function of r at fixed β , i.e.

$$m_{cr}(-r) = -m_{cr}(r). \quad (4.28)$$

Clearly, if we apply R^5 (or R_{sp}^5) twice, we get the identity. Thus, every operator \mathcal{O} can be taken to have a definite R^5 parity

$$\langle \mathcal{O} \rangle |_{m_q, r} \xrightarrow{R_{sp}^5} (-1)^{P_{R^5}^{\mathcal{O}}} \langle \mathcal{O} \rangle |_{-m_q, -r}. \quad (4.29)$$

Let us return to the condition in eq. (4.28). In [2] the authors give two different arguments why this is in fact true, one in perturbation theory and the other in terms of chiral perturbation theory at vanishing pion mass. I

will sketch the second one here, because it is especially easy to understand. However, one should be a bit careful at this point, the definition of the critical mass through the vanishing of the pion mass is not a particularly good choice [24]: in this definition it turns out that the condition in eq. (4.28) is spoiled by cutoff effects, if the quark mass becomes too small. Nevertheless, it has been shown that a (possibly alternative) definition of the critical mass which satisfies eq. (4.28) can always be found [24, 25]. Anyway, such considerations do not affect our study since we do not simulate in that range of the quark mass.

Suppose m_π is proportional to some power of m_q . In a phase with spontaneous chiral symmetry breaking for instance this is true to lowest order in chiral perturbation theory, where we have

$$m_\pi^2 a^2 = a^2 B m_q + \dots \quad (4.30)$$

For the Schwinger model we have the relation $m_\pi \propto m_q^{2/3}$ (see eq. 3.30). The critical mass can thus be defined as the bare mass m_0 where the pion mass m_π vanishes. We determine m_π through decay of the correlation function

$$\begin{aligned} C_{\text{PP}}(x_0, r, m_0) &= a^{d-1} \sum_{\mathbf{x}} \langle P^b(x_0, \mathbf{x}) P^b(0) \rangle |_{r, m_0} \\ &= \frac{a^{d-1}}{\mathcal{Z}} \sum_{\mathbf{x}} \int DU_\mu D\bar{\psi} D\psi P^b(x_0, \mathbf{x}) P^b(0) e^{-S_W} |_{r, m_0}, \end{aligned} \quad (4.31)$$

where P^b is the pseudo scalar density. If one transforms the fields by R^5 and integrates over the transformed fields, one gets

$$C_{\text{PP}}(x_0, r, m_0) = C_{\text{PP}}(x_0, -r, -m_0). \quad (4.32)$$

Since the pion mass is extracted from the exponential decay of C_{PP} , it follows that

$$m_\pi(r, m_0) = m_\pi(-r, -m_0). \quad (4.33)$$

Now, if we choose m_0 such that m_π vanishes, i.e. we set $m_0 = m_{cr}(r)$, then by eq. (4.33) we have $m_\pi(-r, -m_0) = 0$, from which it follows that $-m_0 = m_{cr}(-r)$. So there exists at least one phase, where m_{cr} is odd in r , i.e. $m_0 = m_{cr}(r) = -m_{cr}(-r)$. Hence, under R_{sp}^5 the subtracted mass m_q transforms as follows

$$m_q = m_0 - m_{cr}(r) \xrightarrow{R_{sp}^5} -m_0 - m_{cr}(-r) = -m_q.$$

O(a) Improved Wilson Average

Let \mathcal{O} be a multiplicatively renormalizable operator. Consider the Symanzik expansion of \mathcal{O} in the following form

$$\begin{aligned} \langle \mathcal{O} \rangle |_{r, m_q} &= [\zeta^{\mathcal{O}}(r) + am_q \xi^{\mathcal{O}}(r)] \langle \mathcal{O} \rangle |_{m_q}^{cont} + \\ &+ a \sum_l m_q^{n_l} \eta_{\mathcal{O}_l}^{\mathcal{O}}(r) \langle \mathcal{O}_l \rangle |_{m_q}^{cont} + O(a^2). \end{aligned} \quad (4.34)$$

$\langle \mathcal{O} \rangle |_{r, m_q}$ is the vacuum expectation value of \mathcal{O} taken with the lattice action with Wilson parameter r and subtracted quark mass m_q . The terms $\langle \mathcal{O} \rangle |_{m_q}^{cont}$ appearing on the rhs are the expectation values of continuum operators renormalized at a scale $\frac{1}{a}$. They too have a definite R^5 parity, which is now independent of r

$$\langle \mathcal{O} \rangle |_{m_q}^{cont} = (-1)^{P_{R^5}^{\mathcal{O}}} \langle \mathcal{O} \rangle |_{-m_q}^{cont}. \quad (4.35)$$

In order to link the coefficients in eq. (4.34) to the introduction of the Symanzik expansion in the last section, we remark that here $\zeta^{\mathcal{O}}$ is proportional to the inverse of the renormalization constant $Z_{\mathcal{O}}$ of \mathcal{O} and $\xi^{\mathcal{O}}$ corresponds to $\frac{b_{\mathcal{O}}}{Z_{\mathcal{O}}}$. The sum over l includes all operators with dimension $[\mathcal{O}_l] = [\mathcal{O}] - n_l + 1$ starting from $n_l = 0$, which result from either the insertion of $O(a)$ terms in the action or from the $O(a)$ terms associated with the operator \mathcal{O} itself. In particular for $n_l = 0$ the sum contains the insertion of the clover term

$$c_{sw} \left\langle \int d^d x \bar{\psi}(x) \sigma_{\mu\nu} F_{\mu\nu}(x) \psi(x) \mathcal{O} \right\rangle.$$

Contributions with $n_l = 1$ do not appear in the sum, they are already accounted for in $\xi^{\mathcal{O}}$. The dimension of the operator \mathcal{O} sets an upper bound on the possible n_l .

We do the same expansion for the R_{sp}^5 transformed operator

$$\begin{aligned} \langle \mathcal{O} \rangle |_{-r, -m_q} &= (-1)^{P_{R^5}^{\mathcal{O}}} \langle \mathcal{O} \rangle |_{r, m_q} = \\ &= (-1)^{P_{R^5}^{\mathcal{O}}} [\zeta^{\mathcal{O}}(-r) - am_q \xi^{\mathcal{O}}(-r)] \langle \mathcal{O} \rangle |_{m_q}^{cont} \\ &+ a \sum_l (-1)^{P_{R^5}^{\mathcal{O}_l} + n_l} m_q^{n_l} \eta_{\mathcal{O}_l}^{\mathcal{O}}(-r) \langle \mathcal{O}_l \rangle |_{m_q}^{cont} + O(a^2), \end{aligned} \quad (4.36)$$

where we used eq. (4.29) in the first line and eq. (4.35) in the second. Comparing the two expansions eq. (4.36) and eq. (4.34) order by order in a ,

we find

$$\begin{aligned}
O(1) : \zeta^{\mathcal{O}}(r) - \zeta^{\mathcal{O}}(-r) &= 0 \\
O(a) : am_q [\xi^{\mathcal{O}}(r) + \xi^{\mathcal{O}}(-r)] \langle \mathcal{O} \rangle |_{m_q}^{cont} + \\
a \sum m_q^{n_l} [\eta_{\mathcal{O}_l}^{\mathcal{O}}(r) - (-1)^{n_l + P_{R^5}^{\mathcal{O}_l} + P_{R^5}^{\mathcal{O}}} \eta_{\mathcal{O}_l}^{\mathcal{O}}(-r)] \langle \mathcal{O}_l \rangle |_{m_q}^{cont} &= 0.
\end{aligned} \tag{4.37}$$

Moreover, it has been shown in ref. [2] that

$$n_l + P_{R^5}^{\mathcal{O}_l} + P_{R^5}^{\mathcal{O}} = 1 \pmod{2} \tag{4.38}$$

for any operators \mathcal{O}_l and \mathcal{O} in the expansion. Therefore both $\xi^{\mathcal{O}}$ and $\eta_{\mathcal{O}_l}^{\mathcal{O}}$ are odd in r (the operators in the expansion are assumed to be independent). If we substitute $\langle \mathcal{O} \rangle |_{-r, m_q}$ for $\langle \mathcal{O} \rangle |_{r, m_q}$ in eq. (4.34) and use the above relations, we can define the *Wilson Average* WA of \mathcal{O}

$$\langle \mathcal{O} \rangle |_{m_q}^{WA} \equiv \frac{1}{2} [\langle \mathcal{O} \rangle |_{r, m_q} + \langle \mathcal{O} \rangle |_{-r, m_q}] = \zeta^{\mathcal{O}}(r) \langle \mathcal{O} \rangle |_{m_q}^{cont} + O(a^2). \tag{4.39}$$

which is free of $O(a)$ effects. By applying eq. (4.29) once more in the WA one reaches the equivalent *Mass Average* MA

$$\langle \mathcal{O} \rangle |_{m_q}^{MA} \equiv \frac{1}{2} [\langle \mathcal{O} \rangle |_{r, m_q} + (-1)^{P_{R^5}^{\mathcal{O}}} \langle \mathcal{O} \rangle |_{r, -m_q}] = \zeta^{\mathcal{O}}(r) \langle \mathcal{O} \rangle |_{m_q}^{cont} + O(a^2). \tag{4.40}$$

The Role of Spontaneous Chiral Symmetry Breaking

Let us consider the chiral limit $m_q = 0$ of a theory regularized on the lattice with Wilson fermions. For the continuum limit of such a theory two different scenarios are possible

1. Spontaneous breaking of chiral symmetry does not occur as for instance for QCD in small volume. The theory is analytic at $m_q = 0$ and in eq. (4.34) we can straightaway set the fermion mass to zero. The sum then reduces to the $n_l = 0$ terms and from eq. (4.38) we conclude that the $O(a)$ terms have opposite R^5 parity compared to the leading term in the chiral limit. Thus if \mathcal{O} is even under R^5 , the operators \mathcal{O}_l are odd and their vacuum expectation values vanish in the continuum limit. This is true because of symmetry reasons: R^5 is an element of the chiral group. Also, it follows trivially from equation (4.35). This effect is summarized in the definition of the MA in eq. (4.40), for $P_{R^5}^{\mathcal{O}} = 0 \pmod{2}$ there is no averaging to be done, the expectation value of the operator itself is already $O(a)$ improved.

Conversely, operators odd under R^5 approach their continuum limit with a rate proportional to a . But as we said above their vacuum expectation values are known to vanish in the continuum limit.

2. Chiral symmetry is realized à la Goldstone as is the case for QCD in infinite volume. In this case there is a non-analyticity at $m_q = 0$, the chiral point can only be approached through a limiting procedure. In the continuum theory, while taking the quark mass to zero, the chiral phase is determined by exactly that mass term. If we want to mimic this behavior with Wilson fermions on the lattice, we must make sure that the symmetry breaking effects are determined by the mass- and not by the Wilson term. Strictly speaking, this means that the continuum limit and the chiral limit are no longer interchangeable, one has to take the continuum limit first. In practice one would have to set the parameters such that they obey the condition [2]

$$a\Lambda_{QCD} \ll \frac{m_q}{\Lambda_{QCD}}. \quad (4.41)$$

Here, the factors of Λ_{QCD} merely serve to set the scale and make the quantities dimensionless.

In this case nothing can be said a priori about the order of cutoff effects of vacuum expectation values at vanishing m_q . Still $O(a)$ improved correlation functions can be obtained by calculating Wilson- or mass averages or by employing twisted mass fermions at maximal twist [2].

All these considerations apply to any fermionic theory regularized à la Wilson. We want to numerically test the first scenario described above. As our testing ground, we chose the Schwinger model with two degenerate quark flavors, as we have introduced it in chapter 2. The model seems to be suitable since the R^5 transformation is well defined due to isospin symmetry and more importantly, as a consequence of the Mermin-Wagner theorem [26], continuous chiral symmetry cannot be spontaneously broken in two dimensions. Unfortunately, mainly for numerical reasons, we will not be able to work with massless fermions. Therefore in addition to the $O(a^2)$ cutoff effects expected in the chiral limit, we might observe $O(am_q)$ effects on our quantities.

Chapter 5

Numerical Study

In this chapter we finally turn to the numerical simulation of the Schwinger model. As we have just said above, the goal of the study is to investigate the scaling of Wilson fermions in a framework without spontaneous chiral symmetry breaking.

This chapter is organized in two parts: the first one deals with the algorithm and in the second, we explain the setup of our scaling test and give its results.

5.1 Simulations

We start this section with some algorithmic details of the simulations. We first introduce the algorithm used and then proceed to an analysis of its performance. However, since this was not our main interest, we did not fully explore this subject and can only give a partial analysis here.

5.1.1 Fermion Matrix

So far, we have not yet said, how fermions can be simulated on the lattice: fermion operators anti-commute, so must the fields in the path integral. Hence, they are expressed through anticommuting Grassmann valued fields. On a computer however, it not possible to evaluate such numbers and as a consequence, the fermionic degrees of freedom have to be integrated out in advance.

By applying the integration rules of Grassmann variables to the fermionic part of the partition function \mathcal{Z} , one obtains

$$\int D\bar{\psi}D\psi e^{-\sum_{i,j}\bar{\psi}_i Q_{ij}\psi_j} = \det Q, \quad (5.1)$$

and accordingly for two flavors $(\det Q)^2$. We use the matrix $Q = \gamma_5(D_W + m_0)$ instead of the massive Wilson operator $(D_W + m_0)$. Q is hermitian and because of $\gamma_5^2 = \mathbb{1}$, the determinants of the squared operators are identical. So finally, the partition function which we implemented numerically, is

$$\mathcal{Z} = \int DU_\mu (\det Q[U_\mu])^2 e^{-S_G[U_\mu]} = \int D\phi D\phi^\dagger DU_\mu \exp(-S_G[U_\mu] - \phi^\dagger Q^{-2}\phi). \quad (5.2)$$

In the second step, the fermion determinant was written as

$$(\det Q)^2 = \int D\phi D\phi^\dagger \exp(-\sum_{i,j} \phi_i^\dagger Q_{ij}^{-2} \phi_j), \quad (5.3)$$

with complex scalar fields $\phi(x)$. The ϕ_i are called pseudo fermions [27]. This procedure allows us to sample the determinant stochastically, rather than calculating it exactly.

5.1.2 Hybrid Monte Carlo

We use the hybrid Monte Carlo algorithm [28] in our simulations. It introduces a Hamiltonian

$$H[U_\mu, \Pi_\mu] = \frac{1}{2} \sum_{x,\mu} \Pi_\mu^2(x) + S_G[U_\mu] + \phi^\dagger Q^{-2}\phi, \quad (5.4)$$

by enlarging the system by momenta $\Pi_\mu(x)$ which are conjugate to the gauge fields $ag_0 A_\mu(x)$. A given configuration is evolved in a fictitious time along a trajectory of length τ by integrating Hamilton's equations of motion. This is usually referred to as the molecular dynamics. In order to calculate one trajectory we need the following steps:

1. **Draw momenta randomly** with a Gaussian distribution $P(\Pi_\mu(x)) \propto \exp(-\frac{1}{2}\Pi_\mu^2(x))$.
2. **Heatbath update of the pseudo fermions:** Generate random pseudo fermion fields with the distribution $\exp(-\phi^\dagger Q^{-2}\phi)$. This can be achieved by drawing Gaussian numbers X_i and calculating $\phi = QX$. The X_i are then distributed as required, since $X = Q^{-1}\phi$.
3. **Molecular dynamics:** Hamilton's equations of motion for the gauge fields yield $ag_0 \partial_t A_\mu(x) = \frac{\delta H}{\delta \Pi_\mu(x)} = \Pi_\mu$, or in a discretized form $ag_0 A'_\mu = ag_0 A_\mu + \delta\tau \Pi_\mu + O(\delta\tau^2)$. Thus, the link variables develop like

$$U'_\mu(x) = e^{iag_0 A'_\mu} = \exp(i\Pi_\mu(x)\delta\tau)U_\mu(x). \quad (5.5)$$

The evolution of the momenta is determined through the condition

$$0 = \delta H = \sum_{x,\mu} \Pi_\mu \delta \Pi_\mu + \delta U_\mu F_\mu + F_\mu^\dagger \delta U_\mu^\dagger, \quad (5.6)$$

where we refer to $F_\mu = \frac{\delta S_G}{\delta U_\mu} + \frac{\phi^\dagger \delta Q^{-2} \phi}{\delta U_\mu}$ as the forces. The gauge links U_μ and U_μ^\dagger are treated as independent variables and the variation of the action with respect to the hermitian conjugate variable U_μ^\dagger turns out to be the conjugate of F_μ . For a derivation of the exact expression of the forces see appendix B. Using the infinitesimal form of eq. (5.5) one finds for the variation of the gauge links

$$\delta U_\mu = i \Pi_\mu \delta \tau U_\mu \text{ and } \delta U_\mu^\dagger = -i \Pi_\mu \delta \tau U_\mu^\dagger. \quad (5.7)$$

By inserting these expressions in eq. (5.6) δH becomes

$$\delta H = \sum_{x,\mu} \Pi_\mu [\delta \Pi_\mu + i \delta \tau (U_\mu F_\mu - F_\mu^\dagger U_\mu^\dagger)]. \quad (5.8)$$

Since the momenta Π_μ are finite numbers and independent of each other, the terms inside the square brackets must vanish

$$0 = \delta \Pi_\mu + i \delta \tau (U_\mu F_\mu - F_\mu^\dagger U_\mu^\dagger)$$

and hence, the update of the momenta is given by

$$\Pi'_\mu = \Pi_\mu - i \delta \tau (U_\mu F_\mu - F_\mu^\dagger U_\mu^\dagger). \quad (5.9)$$

4. **Metropolis accept-reject step:** Could we do an exact integration, the energy of the system would not change along a trajectory. But numerical integration introduces discretization errors and we correct for these by a Metropolis accept-reject step at the end of each trajectory

$$P_A([U_\mu, \Pi_\mu] \rightarrow [U'_\mu, \Pi'_\mu]) = \min(1, e^{-\Delta H}), \quad (5.10)$$

where $\Delta H = H([U'_\mu, \Pi'_\mu]) - H([U_\mu, \Pi_\mu])$. The acceptance rate depends thus on the integrator used, large integration errors result in a poor acceptance.

Furthermore, one must use an integrator which is reversible in the sense that

$$P_A([U_\mu, \Pi_\mu] \rightarrow [U'_\mu, \Pi'_\mu]) = P_A([U'_\mu, -\Pi'_\mu] \rightarrow [U_\mu, -\Pi_\mu]).$$

The condition is necessary to prove detailed balance for the algorithm. We use the leapfrog integration scheme, which uses a single step size $\delta \tau$ for both,

momenta and gauge fields. The Π_μ are updated at every half step $(n + \frac{1}{2})\delta\tau$ and the gauge links U_μ at every full step $n\delta\tau$. The pseudo fermions are kept fix along one trajectory. Nevertheless, we need to invert Q^2 at every step to account for the changes of the link variables it depends on. The main computational effort goes into this inversion. We invert the fermion matrix with a conjugate gradient solver.

We implement periodic boundary conditions in space and time direction. Random numbers are generated by Lüscher's RANLUX generator [29]. The code is written in C and parallelized with MPI. The simulations run on 1 to 4 nodes depending on the lattice size, where every node is an ordinary PC with a Pentium4, 2.6 GHz processor. For the production runs we use trajectories of length 1. For the largest lattices at $\beta = 8$ and 12.5, it was necessary to reduce τ during thermalization.

5.1.3 Performance of the Algorithm

Most of the computer time is spent inverting the matrix Q . Therefore the number of calls to the solver needed to produce an independent gauge configuration seems to be a reasonable choice for measuring the performance of the algorithm. We measure this quantity ν by [30]

$$\nu = 2 \left(d\tau^{-1} + 1 \right) \tau_{int}(P) 10^{-3}. \quad (5.11)$$

It is composed of the following factors: the square of the fermion matrix is inverted $(\frac{1}{d\tau} + 1)$ times per trajectory. $\tau_{int}(P)$ is the integrated autocorrelation time of the plaquette, it accounts for the correlation of a sequence of gauge configurations.

Clearly, ν is independent of the computers and the solver used. The lattice parameters, such as the volume V and the quark mass, influence it only by their impact on $\delta\tau$ and the autocorrelation of the system. We give the ν values determined from our simulations in fig. 5.1, the relevant numbers are also collected in table 5.1.

We want to investigate the performance of the code again from a slightly different point of view. We simulate at fixed physical volume. Increasing the lattice size L/a corresponds thus to taking the continuum limit. The overall scaling of the algorithm with L/a can be disentangled into contributions from different sources:

- For the leapfrog integrator the acceptance probability depends on the size of the integration step $\delta\tau$ as

$$\ln P_A \propto V \delta\tau^\alpha,$$

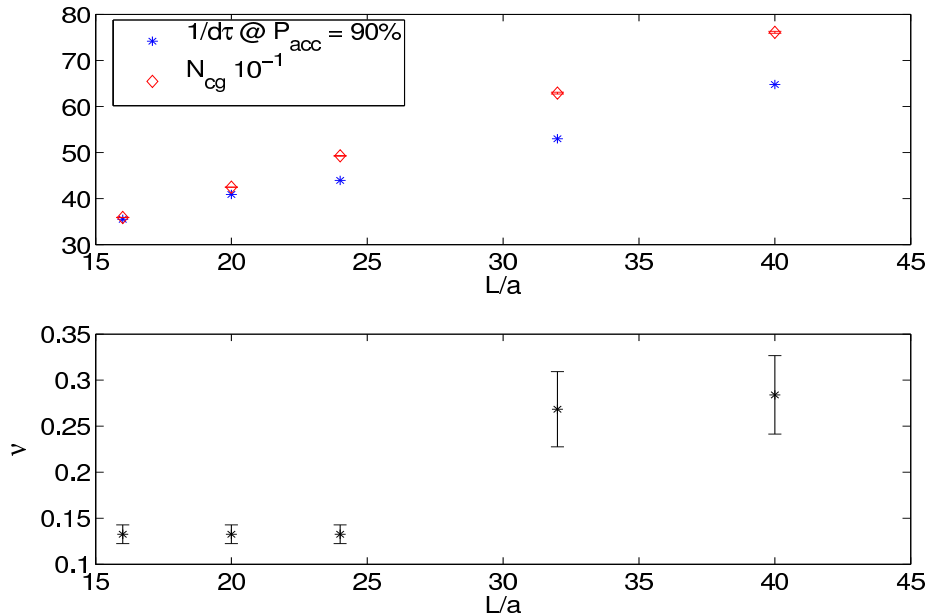


Figure 5.1: Performance of the algorithm: Upper plot: Number of steps necessary in a trajectory of length 1 to reach an acceptance of 90%, and the number of CG iterations as a function of L/a . Below: Measure ν for the number of inversions of the fermion matrix Q needed to calculate an independent gauge configuration.

with $\alpha = 3.4$ [31]. As a consequence, $\delta\tau$ has to be reduced with increasing volume in order to maintain a constant acceptance probability. This behavior is also reflected in the numbers given in table 5.1. We run our simulations at an acceptance of around 90%. In figure 5.1 we give the inverse of the step size rescaled to a constant acceptance of 90%. It increases linearly with the lattice size L/a .

- In the same plot we also show the number of iterations needed in the conjugate gradient solver to reach a residual of $10^{-13}|b|$, where b is the norm of the right hand side of the linear algebra problem to be solved, i.e. $Qx = b$. As one can see, it rises linearly with L/a as well.
- For each iteration in the solver we have to apply Q twice to a vector of length $V \propto L^2$. Since Q is sparse, this scales with the volume of the lattice.
- Finally, one would expect the integrated autocorrelation time of the observables to grow with L/a . Although all the data analysis for this

| L/a | $\tau_{int}(P)$ | $\delta\tau$ | ν | P_{acc} |
|-------|-----------------|--------------|---------|-----------|
| 16 | 1.3(1) | 1/50 | 0.13(1) | 96% |
| 20 | 1.3(1) | 1/50 | 0.13(1) | 94% |
| 24 | 1.3(1) | 1/50 | 0.13(1) | 93% |
| 32 | 2.2(3) | 1/60 | 0.27(4) | 93% |
| 40 | 2.0(3) | 1/70 | 0.28(4) | 92% |

Table 5.1: Number of steps per trajectory and autocorrelation time of the plaquette needed to determine ν for the different lattices. The acceptance probability is also given.

work was done with the method proposed in ref. [32] which calculates autocorrelation times explicitly, no definitive conclusion in this respect could be drawn from the values obtained.

- On the other hand, as a the lattice volume increases, less statistics is necessary to measure an observable with a given precision.

Summing up all these contributions, we would expect the CPU time needed to calculate a given observable to a certain precision to grow as $(L/a)^{4..5}$. Unfortunately, we do not have a reliable measurement of the actual CPU times needed for our simulations to verify this expectation.

We also measure the forces F_μ as derived in appendix B. They drive the evolution of the conjugate momenta Π_μ . As can be seen in the first plot in fig. 5.2, the gauge force increases rather fast with L/a . The reason for this is that F_G is directly proportional to β . This corresponds to an explicit factor of $(L/a)^2$ since we simulate at $\frac{L}{a\sqrt{\beta}} = const$ (see below, in section 5.2.1). In the second plot in fig. 5.2 this factor is divided out. The so scaled gauge force, $F_G^\mu(x)\beta^{-1}$, is equivalent to the sum of the imaginary parts of the staples at the link $U_\mu(x)$. It effectively decreases. In the third plot we give the fermion force eq. (B.5), normalized to its value at the coarsest lattice. The averaged force falls with growing L/a , whereas the maximal force rises. This indicates that the fluctuations of the fermion force become stronger for larger volume.

5.2 Scaling Test

After we have discussed the algorithm, we proceed to the more physical aspects of the simulations. In order to check the argument given in section 4.2.1, we have to do a scaling test. We address this issue in the remaining sections of this work. First, we explain how the continuum limit can be taken in the

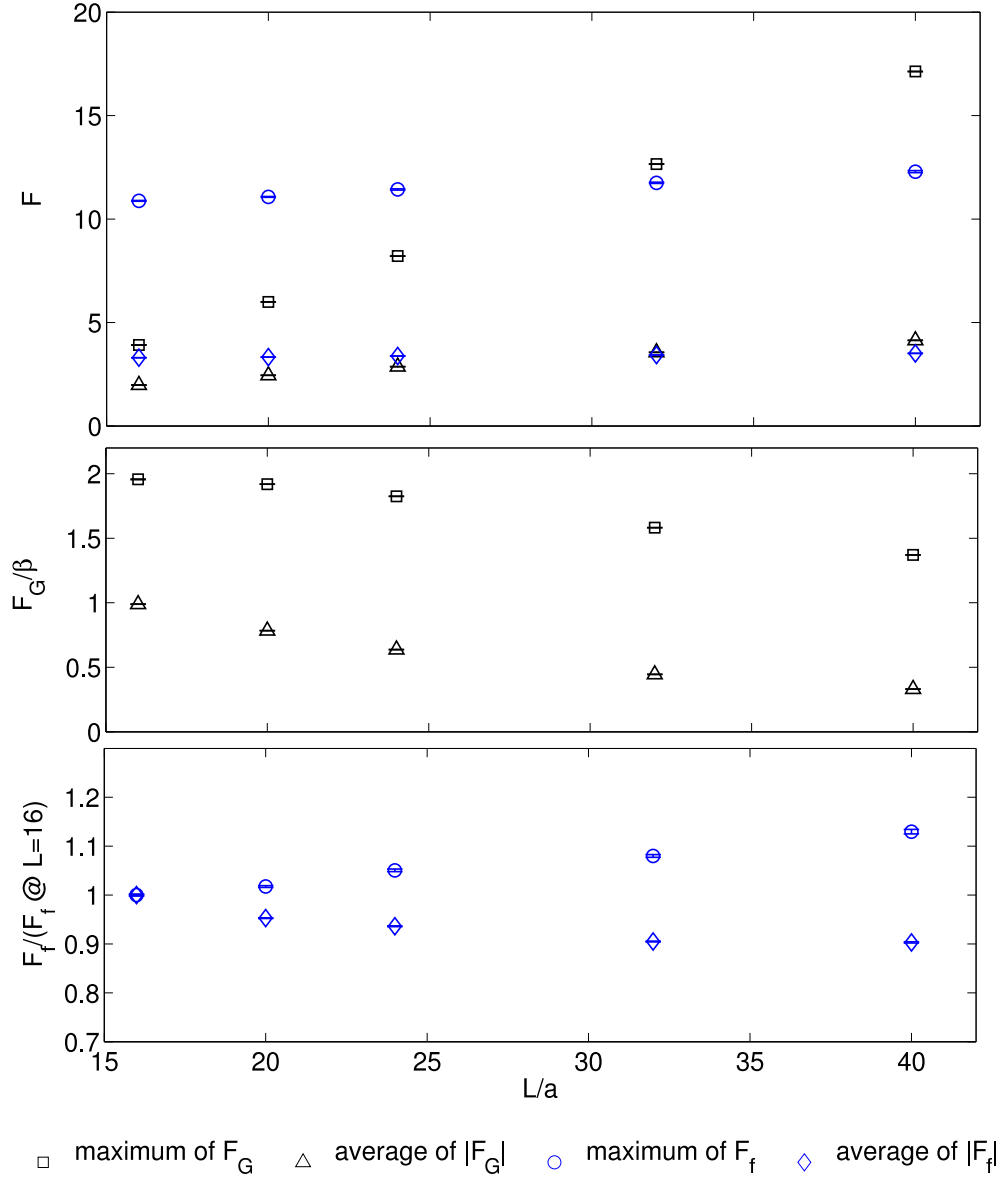


Figure 5.2: The maximal forces and their norm averaged over the volume as a function of L/a . The first plot shows the gauge and fermion forces as defined in appendix B. In the second, the gauge force is scaled by a factor of $\beta \propto (L/a)^2$ and in the third we give the fermion force normalized to its value at the coarsest lattice with $L/a = 16$.

Schwinger model, then we introduce our scaling variables and finally present the numerical results in support of the argument.

5.2.1 Continuum Limit

We want to investigate how physical observables change when we take the lattice spacing to 0. Clearly, this has to be done in a controlled way, we have to make sure that the changes in the scaling observables are merely due to the finer lattice resolution and not to alterations of physical parameters. Furthermore, the simulations are done in a finite volume which we want to keep constant as well. That is, we want to hold the *physical length* L fixed, while changing its discretization length a . Since the coupling constant g_0 of the Schwinger model is dimensionful, it is possible to define such a continuum limit by keeping the dimensionless quantity $g_0 \cdot L = \frac{L}{a\sqrt{\beta}}$ constant [33]. Here, β is the dimensionless coupling introduced in eq. (4.1). In addition, in order to ensure that we simulate at constant physics we have to keep a suitable quark mass m fixed. We define m through the PCAC relation in eq. (2.49) and fix the dimensionless quantity $m \cdot L$ to a constant value. This can be achieved by tuning the hopping parameter κ according to

$$m = \frac{1}{2} \left(\frac{1}{\kappa} - \frac{1}{\kappa_c} \right),$$

where κ_c is defined as the hopping parameter where the quark mass vanishes. Note that due to the super-renormalizability of the Schwinger model we do not have to compute renormalization factors. Indeed, in perturbation theory those are given by an expansion in the coupling

$$Z = (1 + Z^{(1)} a^2 g_0^2 + O(a^4)).$$

The powers of the lattice spacing appear here because g_0 is dimensionful. Since we simulate at fixed g_0 , renormalized operators $\mathcal{O}_R = Z_{\mathcal{O}} \mathcal{O}_0$, differ from the bare ones only by cutoff effects of $O(a^2)$. For the same reason, one could simply set κ_c to 1/4 (see eq. (4.14)) (which anyway we don't do here). Figure 5.3 shows $m \cdot L$ for our simulations as a function of a/L . The relative errors on the PCAC mass are around 1% for all simulations. The values are also collected in table 5.2, together with the corresponding hopping parameter κ , the lattice size L/a , the gauge coupling β and the statistics of the runs. The extent in the time direction is twice the spatial length, such that we have an effective time extension of L/a on the torus. As our coarsest lattice we chose $\beta = 2$ at $L/a = 16$, a parameter set which we also used to compare our results to the ones obtained by Gattringer et al. in ref. [34]. At

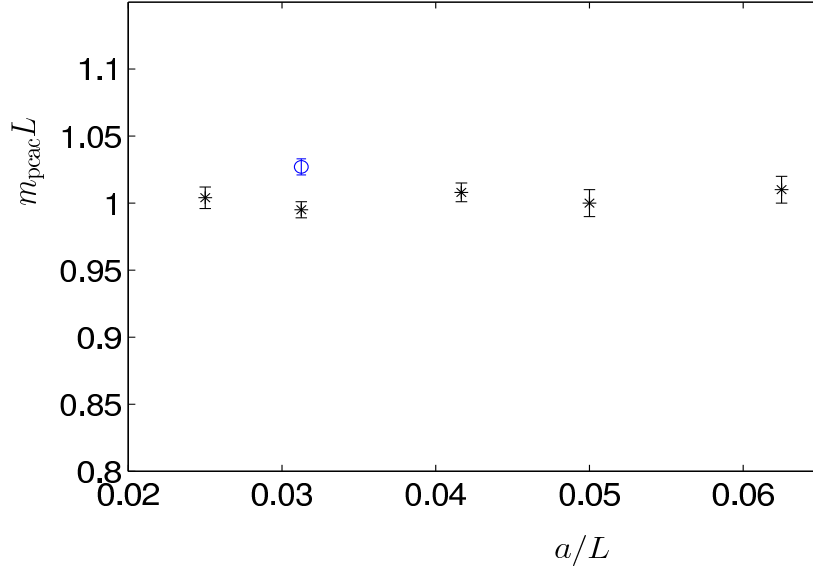


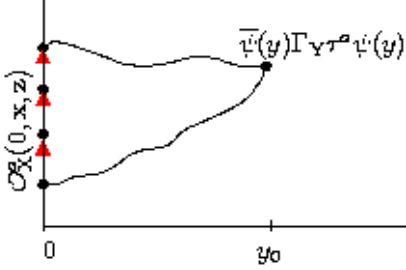
Figure 5.3: Values of $m \cdot L$ for our lattices at the hopping parameters given in table 5.2 as a function of a/L . The circle corresponds to the simulation at $\kappa = 0.2529$ and $L/a = 32$.

$\beta = 8$, we did two simulations with slightly different κ ; the parameters for both of them are given in the table.

| L/a | β | mL | κ | N_{meas} |
|-------|---------|----------|----------|------------|
| 16 | 2 | 1.01(1) | 0.2680 | 5000 |
| 20 | 3.125 | 1.00(1) | 0.2603 | 5000 |
| 24 | 4.5 | 1.008(7) | 0.2564 | 4000 |
| 32 | 8 | 0.995(6) | 0.2530 | 2500 |
| | | 1.027(6) | 0.2529 | 3000 |
| 40 | 12.5 | 1.004(8) | 0.25153 | 1500 |

Table 5.2: Lattice parameters used in the simulations.

5.2.2 Observables



We construct explicit gauge invariant correlation functions from the sources

$$\mathcal{O}_X^a(0, \mathbf{x}, \mathbf{z}) = \bar{\psi}(0, \mathbf{x}) \Gamma_X \tau^a \prod_{i=\mathbf{x}}^{\mathbf{z}-1} U_1(0, i) \psi(0, \mathbf{z}), \quad (5.12)$$

with $X = A$ or P and

$$\Gamma_A = \gamma_0 \gamma_5 \text{ and } \Gamma_P = \gamma_5,$$

while the Pauli matrices τ^a act in flavor space. Thus, the correlators become

$$C_{XY}(y_0) = \frac{1}{12L^3} \sum_{\mathbf{x}, \mathbf{y}, \mathbf{z}} \mathcal{O}_X^a(0, \mathbf{x}, \mathbf{z}) \bar{\psi}(y_0, \mathbf{y}) \Gamma_Y \tau^a \psi(y_0, \mathbf{y}). \quad (5.13)$$

They are projected to zero momentum by summing over spatial indices at the sink. The product of space-like gauge links in \mathcal{O}_X^a enables us to sum over space at the source as well without losing gauge invariance. The additional numerical effort needed is still quite moderate in two dimensions. A more detailed derivation of the correlators can be found in appendix C.

The PCAC mass is also computed from these correlation functions, we calculate the ratio

$$\frac{\partial_0 C_{PA}(x_0)}{2C_{AA}(x_0)} = m \quad (5.14)$$

and average it over a flat region.

The Pion Mass

The π mass can be extracted from both, the pseudo scalar density and the axial current correlator. However, by the procedure introduced in chapter 3, the pseudo scalar density bosonizes to

$$\bar{\psi}^a \gamma_5 \psi^a = \sigma_+^a - \sigma_-^a = \frac{\Lambda}{\pi} \sum_j \sin(\sqrt{4\pi} \phi_j) = \frac{2\Lambda}{\pi} \sin(\sqrt{2\pi} \phi_+) \cos(\sqrt{2\pi} \phi_-)$$

and therefore strongly mixes contributions from the π and the η particle. This behavior is also apparent from the data, as can be seen in figure 5.5. The effective mass determined from the pseudo scalar correlator reaches the common mass plateau only after the one from the axial current. We therefore choose the axial current two-point function to determine the π mass.

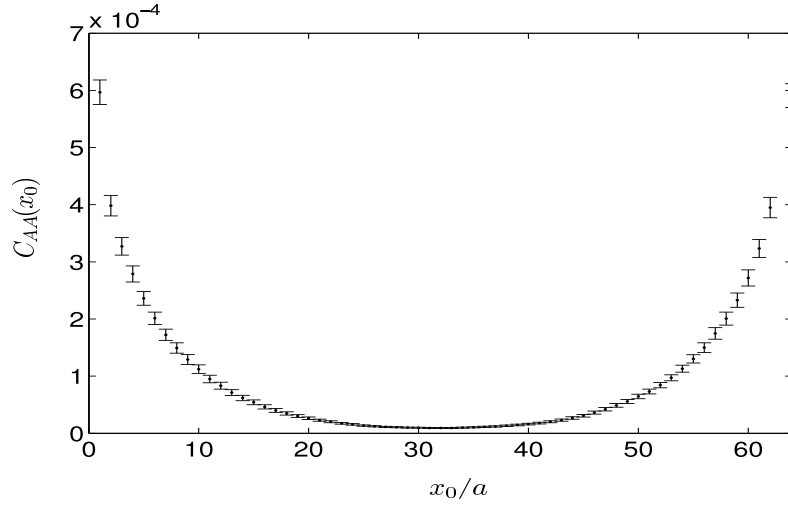


Figure 5.4: Axial current correlator at $\beta = 8$, $\kappa = 0.2530$ and $L/a = 32$.

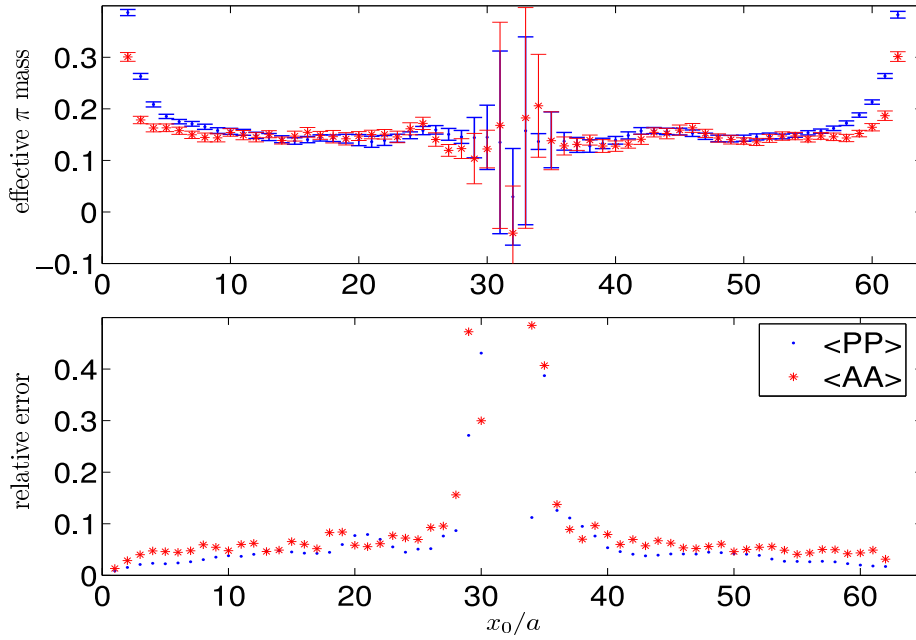


Figure 5.5: Effective π masses from the pseudo scalar density (dots) and the axial current (stars) correlators at $\beta = 8$, $L/a = 32$, $\kappa = 0.2530$.

For x_0 around $T/2$ we assume the correlator $C_{AA}(x_0)$ to be dominated by a single state. In this case, according to eq. (2.11), it should be described by

$$C_{AA}(x_0) = \Phi_\pi^2 \cosh(m_\pi(T/2 - x_0)) \text{ for } x_0 \simeq T/2. \quad (5.15)$$

Indeed, the formula works reasonably well, as is also illustrated by figure 5.4 where we show C_{AA} at $L/a = 32$ as an example. To extract the π mass we define an effective local mass by solving the formula above for m_π and average it over a plateau region on both branches of the cosh. Figure 5.5 shows such an effective mass as a function of x_0/a . The black stars are extracted from $C_{AA}(x_0)$, the blue points from the pseudo scalar density correlator $C_{PP}(x_0)$.

Matrix Element

As we said above, we expect the correlator $C_{XX}(x_0)$ to be proportional to a hyperbolic cosine. Thus, the ratio

$$\frac{C_{XX}(x_0)}{\cosh(m_\pi(T/2 - x_0))} = R(x_0)$$

should be constant around $x_0 = T/2$. In order to estimate it, we use the pion mass m_π previously determined from the same data set as an input. Figure 5.6 shows R for the axial current (above) and the pseudo scalar density (below) for the lattice with $L/a = 32$ at $\kappa = 0.2530$. The square root of R is proportional to a π to vacuum amplitude which in the case of the axial current correlator, corresponds to the analogue of the pion decay constant F_π in QCD

$$\Phi_\pi \equiv \sqrt{\frac{C_{AA}(x_0)}{\cosh(m_\pi(T/2 - x_0))}} \propto \langle 0 | J_0^5 | \pi \rangle. \quad (5.16)$$

We measure Φ_π as a second observable. The value is averaged over the same plateau as the pion mass.

The C_{AA} correlator is clearly even under R^5 , such that by the argument given above in section 4.2.1, we expect the leading cutoff effects to be of $O(a^2)$. As we already said, we use the MATLAB routine provided with ref. [32], for the data analysis. It calculates the integrated autocorrelation time together with the observables. Those are fairly small for both our observables, reaching 1.5 at most. The statistics for the different lattices vary, they are listed in table 5.2. We chose them such that we obtained an error of about 2% on the pion mass. Also, we neglect any finite size effects which we think to be justifiable at a value of $m_\pi \cdot L \approx 4.7$. By the analogy given in chapter 2.1.1, this means that the lattice is almost 5 times larger

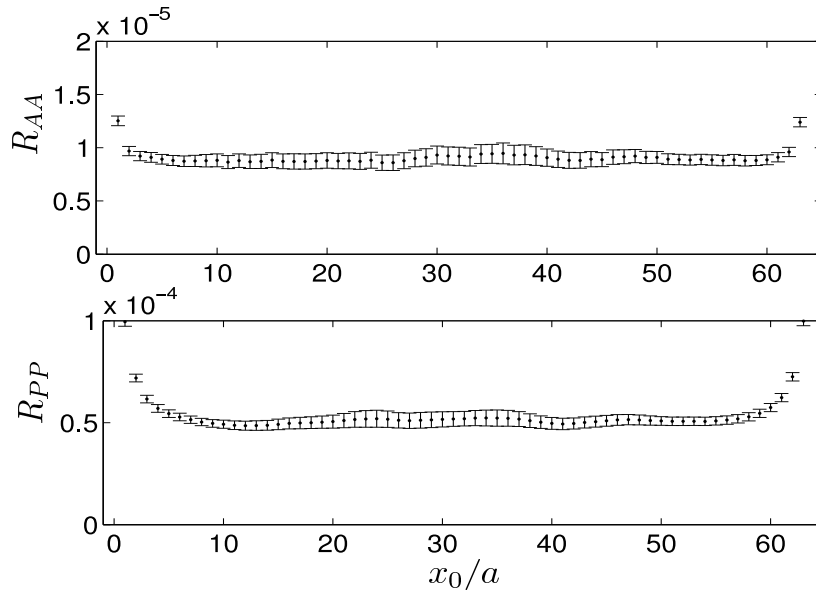


Figure 5.6: Squared matrix elements at $\beta = 8$, $\kappa = 0.2530$ for the pseudo scalar (below) and the axial current (above) two point function.

than the correlation length of the system [35]. In addition since we take the continuum limit in a constant physical volume, any finite size effects should be roughly the same for all lattices.

5.2.3 Results of the Scaling Test

We give the scaling of the dimensionless product $m_\pi \cdot L$ in figure 5.7. The black circle at $L/a = 32$ is from the run at $\kappa = 0.2530$; the diamond is an interpolated value from the two runs at $\kappa = 0.2530$ and $\kappa = 0.2529$. The displacement on the x-axis is for better visibility only. The symbols at $a/L = 0$ correspond to the predictions from the different approximate analytical solutions given in eq. (3.31) obtained at our value of the quark mass. We remind that these solutions are valid in the limit of small fermion masses, more precisely for $m \ll g_0$. We simulate at a ratio of $\frac{m}{g_0} \simeq 0.0886$. We also calculate the ratio

$$A_g = \frac{m_\pi \sqrt{\beta}}{(m\sqrt{\beta})^{2/3}} \quad (5.17)$$

explicitly for all our lattices. From the continuum solutions cited in chapter 3, we expect $A_g \approx 2$, which is indeed the case. The numbers are summarized in table 5.3. We regard the observed consistency as a check of our setup.

| L/a | β | κ | $m_\pi a$ | A_g | $\Phi_\pi a$ |
|-----------|---------|----------|---------------|-----------------|--------------|
| 16 | 2 | 0.2480 | 0.300(4) | 2.06(3) | 0.00250(5) |
| 20 | 3.125 | 0.2603 | 0.236(5) | 2.05(3) | 0.00176(5) |
| 24 | 4.5 | 0.2564 | 0.196(4) | 2.04(3) | 0.00134(3) |
| 32 | 8 | 0.2530 | 0.147(3) | 2.08(4) | 0.00086(3) |
| | | 0.2529 | 0.150(2) | 2.07(3) | 0.00082(2) |
| 40 | 12.5 | 0.25153 | 0.117(2) | 2.04(3) | 0.00067(2) |
| rel.error | | | $\approx 2\%$ | $\approx 2.3\%$ | |

Table 5.3: Simulation results for our observables at five different lattice spacings.

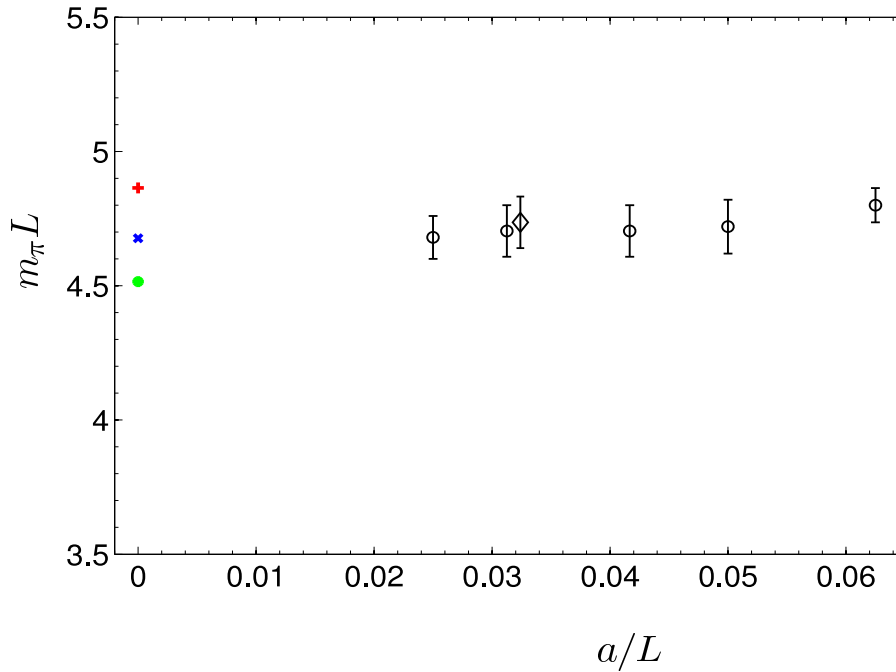


Figure 5.7: Pion mass as a function of a/L . The symbols at $a/L = 0$ are the three values for the approximate continuum solutions given in eq. (3.31), evaluated at our value of the quark mass. The diamond at $L/a = 32$ is an interpolated value from the two runs at $\kappa = 0.2530$ and $\kappa = 0.2529$.

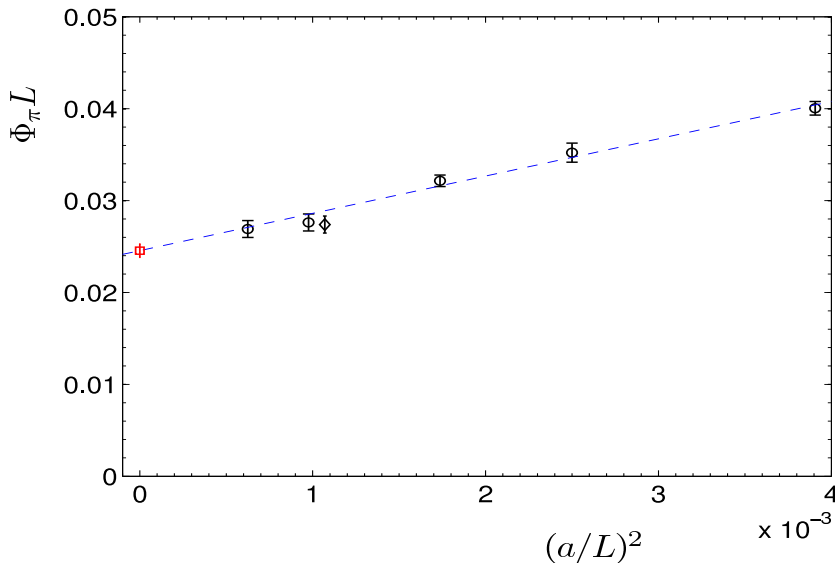


Figure 5.8: Scaling of $\Phi_\pi \cdot L$ as a function of $(a/L)^2$. The square is our continuum limit. The diamond slightly displaced from $L/a = 32$ is an interpolated value from the two runs at $\kappa = 0.2530$ and $\kappa = 0.2529$ respectively. The circle at $L/a = 32$ is from the run with $\kappa = 0.2530$. The interpolated value nearly matches the one from the run at $\kappa = 0.2530$, it does therefore not change our conclusions. The fit parameters given below are calculated with the value at $\kappa = 0.2530$.

It is clear from the plot in fig. 5.7 that within our precision of 2% we do not see any cutoff effects on m_π . In addition, for the same quantity and for a similar choice of parameters, results consistent with lattice artifacts linear in a^2 have been recently reported also in ref. [36].

The discussion of $\Phi_\pi \cdot L$ is a bit more delicate since we see cutoff effects in this quantity. As can be seen from figure 5.8, those are clearly consistent with being linear in a^2 only. However, the argument presented in section 4.2.1 is only valid in the chiral limit. At finite quark mass, one might observe additional effects of $O(am)$. In order to estimate those, we tried to fit the data also to a polynomial with terms linear and quadratic in a . The fit is acceptable in terms of χ^2 and the continuum limit we obtain is in agreement with the one in figure 5.8, but it has a five times larger error. The coefficients of the linear and quadratic terms have large errors as well. They are both consistent with zero, but strongly anti-correlated. We show this fit in figure 5.9, the parameters of both fits are collected in table 5.4. We conclude that the sensitivity of our data to the $O(am)$ effects is very small. Adding a

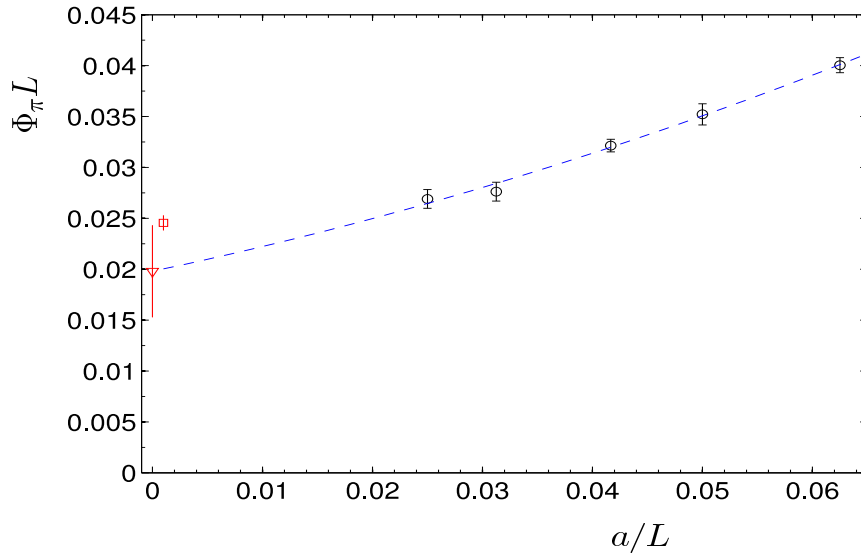


Figure 5.9: The scaling of Φ_π plotted against a/L . The dashed line is a fit to a polynomial with a linear and a quadratic term. At $a/L = 0$ we give the continuum value of this fit (triangle) together with the one obtained from the fit with a term quadratic in a/L only (square).

smaller lattice resolution would probably help to disentangle them from the $O(a^2)$.

| $(a/L)^2$ | (a/L) | continuum limit | χ^2 /dof |
|------------|------------|-----------------|---------------|
| 4.06(31) | | 0.02455(73) | 2.24/3 |
| 1.56(2.35) | 0.23(0.21) | 0.0198(45) | 1.09/2 |

Table 5.4: Fit parameters.

Chapter 6

Conclusions

In this work we argued that in the absence of spontaneous breaking of chiral symmetry, operators even under the R^5 transformation as defined in eq. (4.22) are $O(a)$ improved in the chiral limit. This is the case even if one uses plain Wilson fermions and without including $O(a)$ counterterms. The argument is based on the Symanzik expansion of lattice operators and on spurionic symmetries of the lattice action first considered in ref. [2]. Since R^5 can be constructed from two isovector and one axial isovector rotations, operators even in R^5 are chirally invariant. By the same argument R^5 odd (i.e. chirally non invariant) operators can be shown to approach their continuum limit (vanishing for symmetry reasons) at a rate proportional to a .

We then set out to test the argument numerically. We chose two dimensional QED with two degenerate, dynamical Wilson fermions as our testing field. This model has no $S\chi$ SB due to the Mermin Wagner theorem and it also has the necessary flavor symmetries to construct R^5 . We defined a continuum limit in a finite volume and investigated the scaling of two explicitly R^5 even observables, the mass of the lowest pseudo scalar state π and the pion decay constant of the model Φ_π . Both quantities show, as expected, a scaling consistent with $O(a^2)$, a result which is in agreement also with the recent findings in ref. [36]. However, since for numerical reasons we simulate at finite quark mass, we cannot definitively exclude effects of $O(am)$. In order to assess those quantitatively, it would be necessary to repeat the simulations at different values of the quark mass m . Although they are clearly chirally invariant, both our observables happen to vanish in the chiral limit. It would therefore be very interesting to investigate a quantity which remains finite in that limit. In the Schwinger model, the mass of the isosinglet particle η would meet these requirements. Unfortunately, though we made some first attempts, the calculation of the disconnected diagrams needed for the singlet proved to be very difficult at small fermion mass m . To this end, the

numerical techniques introduced in ref. [37] could provide an efficient way to evaluate the contributions coming from disconnected quark diagrams.

As a byproduct, we also presented some results concerning the performance of the algorithm used in the study.

The main results of this scaling study can be found in a more concise form in ref. [38]. The situation encountered here is very different from QCD in four dimensions (and large volume), where chiral symmetry is spontaneously broken and the $O(a)$ effects for Wilson fermions are rather large [3] and have to be removed by following the Symanzik improvement programme. As a consequence, testing fermionic actions by scaling studies in the Schwinger model provides, in our opinion, very little information about the cutoff effects for the same regularizations in the phenomenologically more relevant case of QCD.

Bibliography

- [1] K. Symanzik. Continuum limit and improved action in lattice theories. 1. Principles and ϕ^4 theory. *Nucl. Phys.*, B226:187, 1983.
- [2] R. Frezzotti and G. C. Rossi. Chirally improving Wilson fermions. I: O(a) improvement. *JHEP*, 08:007, 2004. hep-lat/0306014.
- [3] Martin Lüscher. Advanced lattice QCD. 1998. hep-lat/9802029.
- [4] Stefan Sint. On the Schrödinger functional in QCD. *Nucl. Phys.*, B421: 135–158, 1994. hep-lat/9312079.
- [5] Stefan Sint. The Schrödinger functional with chirally twisted boundary conditions. *PoS (Lat2005) 235*, 2005.
- [6] Julian S. Schwinger. Gauge invariance and mass. II. *Phys. Rev.*, 128: 2425–2429, 1962.
- [7] R.P. Feynman and A. Hibbs. *Quantum mechanics and path integrals*. McGraw-Hill, 1976.
- [8] I. Montvay and G. Münster. *Quantum fields on a lattice*. Cambridge University Press, 1994.
- [9] T.P. Cheng and L.F. Li. *Gauge theory of elementary particle physics*. Oxford University Press, 1984.
- [10] J. Zinn-Justin. *Quantum field theory and critical phenomena*. Oxford University Press, (4. ed.) 2002.
- [11] M.E. Peskin and D.V. Schroeder. *An introduction to quantum field theory*. Westview Press, 1995.
- [12] Kazuo Fujikawa. Comment on chiral and conformal anomalies. *Phys. Rev. Lett.*, 44:1733, 1980.

- [13] S. Elser. *The Local Bosonic Algorithm applied to the massive Schwinger model*. PhD thesis, Humboldt Universität zu Berlin, 2001. hep-lat/0103035.
- [14] S. Ryang. Bosonization in the chiral Schwinger model. *Phys. Rev.*, D35: 3158–3160, 1987.
- [15] Sidney R. Coleman. More about the massive Schwinger model. *Ann. Phys.*, 101:239, 1976.
- [16] Alexei B. Zamolodchikov. Mass scale in the Sine-Gordon model and its reductions. *Int. J. Mod. Phys.*, A10:1125–1150, 1995.
- [17] A. V. Smilga. Critical amplitudes in two-dimensional theories. *Phys. Rev.*, D55:443–447, 1997. hep-th/9607154.
- [18] Kenneth G. Wilson. Confinement of quarks. *Phys. Rev.*, D10:2445–2459, 1974.
- [19] Rajan Gupta. Introduction to lattice QCD. 1997. hep-lat/9807028.
- [20] H. B. Nielsen and M. Ninomiya. No go theorem for regularizing chiral fermions. *Phys. Lett.*, B105:219, 1981.
- [21] Kenneth G. Wilson. Quarks and strings on a lattice. 1975. in: *New Phenomena In Subnuclear Physics. Part A. Proceedings of the First Half of the 1975 International School of Subnuclear Physics, Erice, Sicily.*
- [22] Marco Bochicchio, Luciano Maiani, Guido Martinelli, Gian Carlo Rossi, and Massimo Testa. Chiral symmetry on the lattice with Wilson fermions. *Nucl. Phys.*, B262:331, 1985.
- [23] Martin Lüscher, Stefan Sint, Rainer Sommer, and Peter Weisz. Chiral symmetry and $O(a)$ improvement in lattice QCD. *Nucl. Phys.*, B478: 365–400, 1996. hep-lat/9605038.
- [24] Sinya Aoki and Oliver Bär. Twisted-mass QCD, $O(a)$ improvement and Wilson chiral perturbation theory. *Phys. Rev.*, D70:116011, 2004. hep-lat/0409006.
- [25] R. Frezzotti, G. Martinelli, M. Papinutto, and G. C. Rossi. Reducing cutoff effects in maximally twisted lattice QCD close to the chiral limit. 2005. hep-lat/0503034.

- [26] N. D. Mermin and H. Wagner. Absence of ferromagnetism or antiferromagnetism in one- dimensional or two-dimensional isotropic Heisenberg models. *Phys. Rev. Lett.*, 17:1133–1136, 1966.
- [27] D. H. Weingarten and D. N. Petcher. Monte Carlo integration for lattice gauge theories with fermions. *Phys. Lett.*, B99:333, 1981.
- [28] S. Duane, A. D. Kennedy, B. J. Pendleton, and D. Roweth. Hybrid Monte Carlo. *Phys. Lett.*, B195:216–222, 1987.
- [29] Martin Lüscher. A portable high quality random number generator for lattice field theory simulations. *Comput. Phys. Commun.*, 79:100–110, 1994. hep-lat/9309020.
- [30] Martin Lüscher. Lattice QCD with light Wilson quarks. *PoS*, LAT2005:002, 2005. hep-lat/0509152.
- [31] Rajan Gupta, Gregory W. Kilcup, and Stephen R. Sharpe. Tuning the hybrid Monte Carlo algorithm. *Phys. Rev.*, D38:1278, 1988.
- [32] Ulli Wolff. Monte Carlo errors with less errors. *Comput. Phys. Commun.*, 156:143–153, 2004. hep-lat/0306017.
- [33] Francesco Knechtli and Ulli Wolff. Dynamical fermions as a global correction. *Nucl. Phys.*, B663:3–32, 2003. hep-lat/0303001.
- [34] Christof Gattringer, Ivan Hip, and C. B. Lang. The chiral limit of the two-flavor lattice Schwinger model with Wilson fermions. *Phys. Lett.*, B466:287–292, 1999. hep-lat/9909025.
- [35] M. Lüscher. On a relation between finite size effects and elastic scattering processes. 1983. Lecture given at Cargèse Summer Inst., France.
- [36] N. Christian, K. Jansen, K. Nagai, and B. Pollakowski. Scaling test of fermion actions in the Schwinger model. 2005. hep-lat/0510047.
- [37] Justin Foley et al. Practical all-to-all propagators for lattice QCD. *Comput. Phys. Commun.*, 172:145–162, 2005. hep-lat/0505023.
- [38] Michele Della Morte and Magdalena Luz. Cutoff effects of wilson fermions in the absence of spontaneous chiral symmetry breaking. *Phys. Lett.*, B632:663–666, 2006. hep-lat/0510092.

Appendix A

Conventions

I give here a summary of some conventions used in this work.

A.1 Indices

Unless otherwise stated the letters a, b, c , etc. label flavor indices, Greek letters are Lorentz indices, and space time points are referred to by x, y, z , where we understand x to be the vector $x = (x_0, \mathbf{x})$. For the time component of a x we use either x_0 or t .

A.2 γ Matrices

In two dimensions the γ matrices can be represented by the Pauli matrices. In Minkowski space we choose the following representation:

$$\gamma_0 = \sigma_1 = \begin{pmatrix} 0 & 1 \\ 1 & 0 \end{pmatrix} \quad \gamma_1 = -i\sigma_2 = \begin{pmatrix} 0 & i^2 \\ -i^2 & 0 \end{pmatrix} \quad (\text{A.1})$$

$$\gamma_5 = \gamma_0\gamma_1 = -\sigma_3 = \begin{pmatrix} -1 & 0 \\ 0 & 1 \end{pmatrix}.$$

With this choice the Dirac matrices obey the anti-commutation relation

$$\{\gamma_\mu, \gamma_\nu\} = 2g_{\mu\nu}, \quad (\text{A.2})$$

exactly as in 4 dimensions. The matrix $g_{\mu\nu}$ is the metric in Minkowski space and is given by

$$g = \begin{pmatrix} 1 & 0 \\ 0 & -1 \end{pmatrix}. \quad (\text{A.3})$$

Also in complete analogy to four dimensional Minkowski space γ_0 and γ_5 are hermitian, whereas γ_1 is anti hermitian.

A.2.1 Euclidean γ Matrices

The Euclidean matrices are obtained from the Minkowskian by

$$\gamma_0^E = \gamma_0 = \sigma_1 = \begin{pmatrix} 0 & 1 \\ 1 & 0 \end{pmatrix} \quad \gamma_1^E = -i\gamma_1 = -\sigma_2 = \begin{pmatrix} 0 & i \\ -i & 0 \end{pmatrix} \quad (\text{A.4})$$

and

$$\gamma_5^E = i\gamma_0^E\gamma_1^E = -\sigma_3. \quad (\text{A.5})$$

All matrices are hermitian and eq. (2.6) follows directly from the properties of the Pauli matrices.

Appendix B

Calculation of the Forces

Gauge Force

$$\begin{aligned}
\frac{\delta S_G}{\delta U_\mu(x)} &= -\frac{\beta}{2} \frac{\delta}{\delta U_\mu(x)} \sum_y W_{\mu\nu}(y) + W_{\mu\nu}^\dagger(y) = \\
&= -\frac{\beta}{2} [U_\nu(x + \hat{\mu})U_\mu^\dagger(x + \hat{\nu})U_\nu^\dagger(x) + \\
&\quad + U_\nu^\dagger(x + \hat{\mu} - \hat{\nu})U_\mu^\dagger(x - \hat{\nu})U_\nu(x - \hat{\nu})]
\end{aligned} \tag{B.1}$$

Varying with respect to U_μ^\dagger , we get the hermitian conjugate of the above expression. So, the part of $[U_\mu F_\mu - h.c.]$ resulting from the gauge action is

$$\begin{aligned}
&-\frac{\beta}{2} [W_{\mu\nu}(x) + W_{\mu\nu}^\dagger(x - \hat{\nu}) - W_{\mu\nu}(x - \hat{\nu}) - W_{\mu\nu}^\dagger(x)] = \\
&= -i\beta [\text{Im } W_{\mu\nu}(x) - \text{Im } W_{\mu\nu}(x - \hat{\nu})].
\end{aligned} \tag{B.2}$$

Fermion Force

For the fermion force we have to calculate the variation of the inverse Q^{-N_f} . This can be done through the following trick. Since $Q^{N_f}Q^{-N_f} = \mathbf{1}$ we have

$$0 = \frac{\delta}{\delta U_\mu}(Q^{N_f}Q^{-N_f}) = \left(\frac{\delta Q^{N_f}}{\delta U_\mu}\right)Q^{-N_f} + Q^{N_f}\left(\frac{\delta Q^{-N_f}}{\delta U_\mu}\right).$$

and by multiplying with Q^{-N_f} from the left we get

$$\frac{\delta Q^{-N_f}}{\delta U_\mu(y)} = -Q^{-N_f} \frac{\delta Q^{N_f}}{\delta U_\mu(y)} Q^{-N_f}.$$

We use the fermion matrix in the form (4.15) to calculate the variation of Q^2 explicitly. We write space time points as arguments and Lorentz indices

as Greek indices,

$$\begin{aligned}
& \frac{\delta}{\delta U_\mu(x)} \sum_{\beta,j} Q_{\alpha,\beta}(i,j) Q_{\beta,\gamma}(j,k) = \\
& = -\kappa \sum_{\beta} [(r - \gamma_\mu)\gamma_5]_{\alpha,\beta} \delta(i,x) Q_{\beta,\gamma}(x + \hat{\mu}, k) + \\
& \quad + Q_{\alpha,\beta}(i,x) [(r - \gamma_\mu)\gamma_5]_{\beta,\gamma} \delta(k, x + \hat{\mu})
\end{aligned} \tag{B.3}$$

and

$$\begin{aligned}
& \frac{\delta}{\delta U_\mu^\dagger(x)} \sum_{\beta,j} Q_{\alpha,\beta}(i,j) Q_{\beta,\gamma}(j,k) = \\
& = -\kappa \sum_{\beta} [(r + \gamma_\mu)\gamma_5]_{\alpha,\beta} \delta(i - \hat{\mu}, x) Q_{\beta,\gamma}(i - \hat{\mu}, k) + \\
& \quad + Q_{\alpha,\beta}(i, k + \hat{\mu}) [(r + \gamma_\mu)\gamma_5]_{\beta,\gamma} \delta(k, x).
\end{aligned} \tag{B.4}$$

So finally the contribution to $(U_\mu F_\mu - h.c.)$ of the Fermion matrix equals (double indices are summed over)

$$\begin{aligned}
& -2i \operatorname{Im} \left\{ (Q^{-2}\phi)_\alpha^\dagger(x) [-\kappa(r - \gamma_\mu)\gamma_5 U_\mu(x)]_{\alpha,\beta} Q_{\beta,\gamma}(x + \hat{\mu}, k) (Q^{-2}\phi)_\gamma(k) + \right. \\
& \quad \left. + (Q^{-2}\phi)_\alpha^\dagger(i) Q_{\alpha,\beta}(i, x) [-\kappa(r - \gamma_\mu)\gamma_5 U_\mu(x)]_{\beta,\gamma} (Q^{-2}\phi)_\gamma(x + \hat{\mu}) \right\} \\
& = -2i \operatorname{Im} \left\{ (Q^{-1}\phi)_\alpha^*(x) [-\kappa(r - \gamma_\mu)\gamma_5 U_\mu(x)]_{\alpha,\beta} (Q^{-2}\phi)_\beta(x + \hat{\mu}) + \right. \\
& \quad \left. + (Q^{-2}\phi)_\alpha^*(x) [-\kappa(r - \gamma_\mu)\gamma_5 U_\mu(x)]_{\alpha,\beta} (Q^{-1}\phi)_\beta(x + \hat{\mu}) \right\}.
\end{aligned} \tag{B.5}$$

Appendix C

Correlation Functions and Topological Charge

C.1 Correlation Functions

In order to evaluate the meson masses we need to calculate correlation functions of meson operators $\mathcal{O} = \bar{\psi}(x)\Gamma T\psi(y)$, where Γ stands for the Dirac structure of the operator and T is a flavor matrix, or $\mathbf{1}$ for the singlet. We calculate gauge invariant point to point correlators given by

$$\begin{aligned}
C_{T\Gamma T'\Gamma'}(x^0, z^0, y) &= \\
&= \left\langle \sum_{abcd} \sum_{\alpha\beta\gamma\delta} \bar{\psi}(x^0)_\alpha^a \Gamma_{\alpha\beta} T^{ab} \prod_{i=\mathbf{x}}^{z-1} U_1(0, i) \psi_\beta^b(z^0) \bar{\psi}_\gamma^c(y) \Gamma'_{\gamma\delta} T'^{cd} \psi_\delta^d(y) \right\rangle = \\
&= - \sum_{abcd} \sum_{\alpha\beta\gamma\delta} \Gamma_{\alpha\beta} T^{ab} \Gamma'_{\gamma\delta} T'^{cd} \left\langle \prod_{i=\mathbf{x}}^{z-1} U_1(0, i) \psi_\beta^b(z^0) \bar{\psi}_\gamma^c(y) \psi_\delta^d(y) \bar{\psi}_\alpha^a(x^0) \right\rangle = \\
&= \sum_{abdc} \sum_{\alpha\beta\gamma\delta} \Gamma_{\alpha\beta} T^{ab} \Gamma'_{\gamma\delta} T'^{cd} \prod_{i=\mathbf{x}}^{z-1} U_1(0, i) [S_{\delta\gamma}^{dc}(y, y) S_{\beta\alpha}^{ba}(x^0, z^0) - \\
&\quad S_{\beta\gamma}^{bc}(z^0, y) S_{\delta\alpha}^{da}(y, x^0)]
\end{aligned} \tag{C.1}$$

where in the last step the Wick contractions were evaluated. $S(x, y)$ is the Fermion propagator and we use $x^0 = (0, \mathbf{x})$ and $z^0 = (0, \mathbf{z})$ to remind that they are both on the same $t = 0$ timeslice. The product of space like gauge links leading from x^0 to z^0 makes the correlator gauge invariant. Periodic boundary conditions allow us to use the product of $\prod U_1$ rather than $\prod U_1^\dagger$ even in the case $\mathbf{x} > \mathbf{z}$. For Wilson fermions the propagator is diagonal in

flavor and the flavor structure can be evaluated separately

$$C_{\Gamma\Gamma'}(x^0, z^0, y) = \sum_{\alpha\beta\gamma\delta} (\text{tr } T)^2 S_{\delta\gamma}(y, y) \Gamma'_{\gamma\delta} S_{\beta\alpha}(x^0, z^0) \Gamma_{\alpha\beta} \prod_{i=\mathbf{x}}^{z-1} U_1(0, i) - (\text{tr } T^2) S_{\beta\gamma}(z^0, y) \Gamma'_{\gamma\delta} S_{\delta\alpha}(y, x^0) \Gamma_{\alpha\beta} \prod_{i=\mathbf{x}}^{z-1} U_1(0, i). \quad (\text{C.2})$$

We project to zero momentum by summing over the spatial indices at the sink y and average over the timeslice at the source.

$$C_{\Gamma\Gamma'}(y_0) = \frac{1}{3L^3} \sum_{\mathbf{y}, \mathbf{x}, \mathbf{z}} C_{\Gamma\Gamma'}(x^0, z^0, y) \quad (\text{C.3})$$

We use

$$QS = \gamma_5(D_w + m_0)S = \mathbb{1}\gamma_5,$$

$$S = Q^{-1}\gamma_5$$

to express the propagator through the fermion matrix.

C.1.1 Flavor Triplet

For the flavor triplet $T = \frac{\tau^a}{2}$ with a traceless Pauli matrix τ^a , there are no disconnected parts. The factor $6/12$ includes the flavor trace and the average over the isospin components. The correlation functions become

$$C_{\Gamma\Gamma'}(y_0) = -\frac{6}{12L^3} \sum_{\mathbf{x}, \mathbf{y}, \mathbf{z}} \sum_{\alpha\beta\gamma\delta} S_{\beta\gamma}(z^0, y) \Gamma'_{\gamma\delta} S_{\delta\alpha}(y, x^0) \prod_{i=\mathbf{x}}^{z-1} U_1(0, i) \Gamma_{\alpha\beta}. \quad (\text{C.4})$$

We define

$$\bar{S}(y) = \sum_{\mathbf{x}} S(x, y) \prod_{i=\mathbf{w}}^{x-1} U_1(0, i), \quad (\text{C.5})$$

where \mathbf{w} is an arbitrary point at the timeslice of the source. Using the γ_5 hermiticity of \bar{S} we get from (C.4)

$$C_{\Gamma\Gamma'}(y_0) = -\frac{1}{2L^3} \sum_{\mathbf{y}} \sum_{\alpha\beta\gamma\delta} \bar{S}_{\beta\gamma}(y) (\Gamma' \gamma_5)_{\gamma\delta} \bar{S}_{\delta\alpha}^\dagger(y) (\gamma_5 \Gamma)_{\alpha\beta}. \quad (\text{C.6})$$

In order to extract the PCAC and the pion mass, we need the following correlation functions:

- **PP correlator:** $\frac{1}{3}\langle\bar{\psi}\gamma_5\frac{\tau^a}{2}\psi\bar{\psi}\gamma_5\frac{\tau^a}{2}\psi\rangle$

For the pseudo scalar density $\Gamma = \Gamma' = \gamma_5$ and

$$\begin{aligned} C_{\text{PP}}(y_0) &= -\frac{1}{2L^3}\sum_{\mathbf{y}}\sum_{\beta\delta}\bar{S}_{\beta\delta}(y)\bar{S}_{\delta\beta}^\dagger(y) = \\ &= -\frac{1}{2L^3}\sum_{\mathbf{y}}\sum_{\beta\delta}\bar{S}_{\beta\delta}(y)\bar{S}_{\beta\delta}^*(y). \end{aligned} \quad (\text{C.7})$$

We have to solve the linear problem

$$Q_{\alpha\beta}(x,y)\bar{S}_{\beta\gamma}(y) = (\gamma_5)_{\alpha\gamma}\left(\delta_{y_0,0}\prod_{i=0}^{\mathbf{x}}U_1(i)\right).$$

The inversions for the two Dirac components are done separately.

- **A₀A₀ correlator:** $\frac{1}{3}\langle\bar{\psi}\gamma_0\gamma_5\frac{\tau^a}{2}\psi\bar{\psi}\gamma_0\gamma_5\frac{\tau^a}{2}\psi\rangle$

In this case $\Gamma = \Gamma' = \gamma_0\gamma_5$,

$$\begin{aligned} C_{\text{AA}}(y_0) &= \frac{1}{2L^3}\sum_{\mathbf{y}}\sum_{\beta\delta}[\bar{S}\gamma_0]_{\beta\delta}(y)[\bar{S}^\dagger\gamma_0]_{\delta\beta}(y) = \\ &= \frac{1}{2L^3}\sum_{\mathbf{y}}\sum_{\beta\delta}[\bar{S}\gamma_0]_{\beta\delta}(y)[\gamma_0\bar{S}]_{\delta\beta}^\dagger(y) = \\ &= \frac{1}{2L^3}\sum_{\mathbf{y}}\sum_{\beta\delta}[\bar{S}\gamma_0]_{\beta\delta}(y)[\gamma_0\bar{S}]_{\beta\delta}^*(y). \end{aligned} \quad (\text{C.8})$$

Since $\gamma_0 = \sigma_1$, $(\gamma_0\bar{S})$ and $(\bar{S}\gamma_0)$ are the row and the column permutation of \bar{S} . The A_0A_0 correlator can thus be constructed from \bar{S} and we need no additional inversion.

- **PA₀ correlator:** $\frac{1}{3}\langle\bar{\psi}\gamma_5\frac{\tau^a}{2}\psi\bar{\psi}\gamma_0\gamma_5\frac{\tau^a}{2}\psi\rangle$

In this case we have $\Gamma = \gamma_5$ and $\Gamma' = \gamma_0\gamma_5$ and

$$\begin{aligned} C_{\text{PA}}(y_0) &= -\frac{1}{2L^3}\sum_{\mathbf{y}}\sum_{\beta\delta}[\bar{S}\gamma_0]_{\beta\delta}(y)\bar{S}_{\delta\beta}^\dagger(y) = \\ &= -\frac{1}{2L^3}\sum_{\mathbf{y}}\sum_{\beta\delta}[\bar{S}\gamma_0]_{\beta\delta}(y)\bar{S}_{\beta\delta}^*(y). \end{aligned} \quad (\text{C.9})$$

| | | |
|----------------|--------------------------|--------------------------|
| \bar{S}_{11} | $[\bar{S}\gamma_0]_{12}$ | $[\gamma_0\bar{S}]_{21}$ |
| \bar{S}_{12} | $[\bar{S}\gamma_0]_{11}$ | $[\gamma_0\bar{S}]_{22}$ |
| \bar{S}_{21} | $[\bar{S}\gamma_0]_{22}$ | $[\gamma_0\bar{S}]_{11}$ |
| \bar{S}_{22} | $[\bar{S}\gamma_0]_{21}$ | $[\gamma_0\bar{S}]_{12}$ |

Table C.1: Elements of the Fermion propagator \bar{S} and corresponding elements of $\gamma_0\bar{S}$ and $\bar{S}\gamma_0$ respectively.

C.1.2 Flavor Singlet

For the flavor singlet $T = 1/2$, there are contributions from the disconnected parts.

$$C_{\Gamma\Gamma'}^{singlet}(y_0) = C_{\Gamma\Gamma'}^{triplet} + \frac{1}{L^3} \sum_{\mathbf{x}_0, \beta} [S\Gamma']_{\beta\beta}(x_0, x_0) \sum_{\mathbf{y}, \alpha} [S\Gamma]_{\alpha\alpha}(y, y) \quad (C.10)$$

Noisy Estimators

We calculate the disconnected diagrams using noisy estimators: Let χ be a noise vector (Gaussian or Z_2) such that for every two components χ_x and χ_y

$$\langle \chi_x^* | \chi_y \rangle_\chi = \delta_{x,y} \text{ and } \langle \chi_x \rangle_\chi = 0$$

then

$$Q_{\alpha\beta}^{-1}(x, y) = \langle \chi_y^* | \sum_z Q_{\alpha\beta}^{-1}(x, z) \chi_z \rangle = \sum_z Q_{\alpha\beta}^{-1}(x, z) \delta_{y,z}. \quad (C.11)$$

If the flavor structure is not diagonal the inversion has to be done for every flavor component separately. On the other hand, if the flavor structure is diagonal, we can use noisy estimators such that $\langle \chi_\alpha^*(x) | \chi_\beta(y) \rangle = \delta_{x,y} \delta_{\alpha,\beta}$. We make use of this fact by extracting the singlet mass from the PP correlator.

- **PP Correlator:** $\frac{1}{4} \langle \bar{\psi} \gamma_5 \psi \bar{\psi} \gamma_5 \psi \rangle$

Since for this correlator $QS\gamma_5 = \gamma_5^2 = \mathbf{1}$, we solve the problem

$$Q^{\alpha\beta}(x, y) A^\beta(y) = \chi^\alpha(x)$$

for $A^\beta(y)$. This yields

$$C_{\text{PP}}^{singlet}(y_0) = C_{\text{PP}}^{triplet}(y_0) + \frac{1}{L^3} \left(\sum_{\mathbf{x}^0, \gamma} \chi_\gamma^*(x^0) \sum_{\mathbf{z}, \epsilon} Q_{\gamma\epsilon}^{-1}(x^0, z^0) \chi_\epsilon(z^0) \right) \cdot \left(\sum_{\mathbf{x}\alpha} \chi_\alpha^*(x) \sum_{\mathbf{y}\beta} Q_{\alpha\beta}^{-1}(x, y) \chi_\beta(y) \right). \quad (C.12)$$

C.2 Topological Charge

On the lattice, the topological charge ν can be defined by

$$\nu = \frac{1}{2\pi} \sum_{\text{p}} \phi_{\text{p}}, \quad (\text{C.13})$$

where p runs over all plaquettes and $\phi_{\text{p}} = \text{Im} \ln(W_{\mu\nu})$ is the phase of the plaquette. ν is always an integer. This definition follows from eq. (4.3) and the expression of the topological charge in the continuum eq. (2.58).

The topological susceptibility is

$$\chi = \frac{1}{N_p} (\langle \nu^2 \rangle - \langle \nu \rangle^2). \quad (\text{C.14})$$

Selbständigkeitserklärung

Hiermit erkläre ich, die vorliegende Arbeit selbständig ohne fremde Hilfe verfaßt und nur die angegebene Literatur und Hilfsmittel verwendet zu haben.

Magdalena Luz

23. November 2005